Major Research Project

Molecular and Cellular Life Sciences MSc

The Role of Ninein in the Regulation of Microtubule Organization at the Centrosome

Arianna Sandron, Fangrui Chen, Anna Akhmanova

Division of Cell Biology, Neurobiology and Biophysics

Faculty of Science

Universiteit Utrecht

Layman's Summary

Cells can move, change their shape, divide and transport compounds across different compartments by using a system of dynamic protein filaments named "microtubules". The organization in space and time of microtubules, crucial for the cell to adapt to a variety of external stimuli, is a delicate activity which primarily depends on a special organelle, the centrosome. Here, new microtubules are constantly assembled and subsequently attached in order to ensure the formation of a normal microtubule network. These processes are finely regulated by an impressive number of proteins at the centrosome; most of these proteins are known, but their precise function, together with the underlying mechanisms, remains to be explained and requires further research.

In this project, we used genome-editing techniques and cell biology experiments to investigate the function of a centrosomal protein, Ninein, and its involvement in the regulation of microtubules inside the cell. We identified the specific protein region that is responsible for Ninein's localization at the centrosome, and we demonstrated that the presence of Ninein is required to guarantee the proper attachment of microtubules at the centrosome. Moreover, we showed that Ninein does not cover a role in the construction of new microtubules, and that, consistently, Ninein is not able to interact with complexes involved in this process. Finally, we observed that the presence at the centrosome of another protein, CLASP2, depends on Ninein, and that these two proteins are able to bind to each other through specific regions.

Overall, the results showed in this report helped to gather new insights on the contribution of Ninein in the process of microtubule organization at the centrosome. Additional studies are still needed to understand the complexity of microtubule dynamics, and remain essential to improve our understanding and treatment of many centrosome-related pathologies, which also include several types of cancer.

Contents

1. Summary

Many fundamental cellular processes, such as the transport of intracellular cargos and the segregation of mitotic chromosomes, depend on the spatiotemporal regulation of microtubule networks. Specific subcellular compartments, named Microtubule Organizing Centers (MTOCs), are involved in this crucial and delicate function by controlling microtubule nucleation and anchoring. The centrosome represents the major MTOC of eukaryotic cells, and it is composed of a pair of orthogonal centrioles surrounded by the highly dense and protein-rich pericentriolar material (PCM). The PCM proteins can interact directly and indirectly with nucleating complexes and with newly made microtubules, thus promoting nucleation and ensuring microtubule anchoring. In which way many of these proteins fulfill these functions is, however, currently poorly understood. Further studies are therefore needed in order to elucidate more precisely the dynamics of centrosomal microtubule organization.

In this project, we employed CRISPR/Cas9 genome editing technology and Knock-Down via RNA interference to investigate the role of Ninein, a protein resident on the mother centriole, in the regulation of microtubule organization. Ninein is known to be essential for proper anchoring of microtubules, but the mechanism underlying its role are still not known. Whether Ninein can cover a role in microtubule nucleation remains as well to be determined.

We show that Ninein localizes to the centrosome through its C-terminal domain and that its depletion severely impairs the normal microtubule density at the centrosome. Importantly, we demonstrate that Ninein and γ-tubulin do not interact, and that γ-tubulin levels at the centrosome are not affected by Ninein's depletion. We found that the late stage of microtubule regrowth, but not the early one, is impaired in the absence of Ninein. Finally, we demonstrate that CLASP2 levels at the centrosome are dramatically decreased in Ninein Knockout cells, and that Ninein binds to the C-terminal domain of CLASP2 trough a coiled-coil domain located in the 601-1050 amino acidic region.

In conclusion, by providing information about the contribution of Ninein to the processes of microtubule nucleation and anchoring, our work helped to gain new insights in the regulation of microtubule organization at the centrosome.

2. Introduction

2.1 Microtubules and Microtubule Organizing Centers (MTOC)

Microtubules are dynamic components of the cytoskeleton involved in various crucial cellular functions, such as intracellular transport of cargos, chromosome separation and regulation of cell polarity and motility (Martin and Akhmanova, 2018; Wu and Akhmanova, 2017). Microtubule arrays can be shaped in different patterns in order to adapt to cell cycle phases and cell function (e.g.: neurons and epithelial cells) (Sanchez and Feldman, 2017). The regulation of microtubule networks in space and time is therefore a crucial task, performed inside the cell by structures named Microtubule Organizing Centers (MTOCs). MTOCs are composed of protein complexes that function in the regulation of microtubules' nucleation, anchoring and stabilization. Although many cellular compartments, included the cell cortex and the Golgi apparatus, are known to act as MTOCs, the title of "major MTOCs" in eukaryotic cells has traditionally been given to the centrosome.

2.2 The Centrosome

The centrosome is a multifunctional organelle, implicated in a range of diverse and important processes inside the cell: it is required for an efficient and fast chromosome segregation, it regulates processes like ciliogenesis and cell polarity and it influences organelle transport and positioning (Bornens, 2012; Goodson and Jonasson, 2018; Meraldi, 2016; Reiter and Leroux, 2017; Sánchez and Dynlacht, 2016; Vertii et al., 2016). The regulation of specific signaling pathways, the response to DNA damages and the organization of actin filaments, are also part of the centrosome's duties (Arquint et al., 2014; Farina et al., 2016; Mullee and Morrison, 2016; Schatten, 2008).

The use of electron microscopy, together with super resolution microscopy and proteomics studies, has helped through time to uncover the structure of the centrosome, which is now very well-known (Andersen et al., 2003; Bernhard & De Harven, 1956; Gupta et al., 2015; Gould & Borisy, 1977; Lawo et al., 2012; Mennella et al., 2012): the centrosome is a membrane-less self-assembling organelle, composed of a pair of orthogonal microtubule-based centrioles surrounded by the protein-rich pericentriolar material (in short PCM) (Paz and Lüders, 2018; Woodruff et al., 2017).

2.2.1 Centrioles

More into detail, the centrioles are cylindric structures that are found, aside from the centrosome, also at the base of cilia and flagella. The outside region of the centriole is composed of nine triplets of microtubules, whereas the inner region, which helps to connect and maintain in position the triplets, is occupied by a cartwheel structure, formed by a central hub surrounded by nine spokes that end with pinheads (Avidor-Reiss and Gopalakrishnan, 2013; Azimzadeh and Marshall, 2010). In addition, the older centriole, named "mother" centriole, is decorated at the distal end by other two symmetric structural features: the distal appendages, involved in ciliogenesis, and the subdistal appendages, which are used to anchor microtubules at the centrosome and can only be found in animal cells (Azimzadeh and Marshall, 2010; Mogensen et al., 2000). On the other hand, these appendages are not found in the "daughter" centriole.

2.2.2 Pericentriolar Material (PCM)

The establishment of multivalent and hierarchical interactions between various proteins results in the formation of a highly dynamic and electron-dense matrix around the centrioles: the Pericentriolar material (PCM; Figure 1) (Lawo et al., 2012). In the PCM, proteins are precisely disposed in a toroidal manner (Lawo et al., 2012; Mennella et al., 2012); one of the most important actors in the organization of this structure is Pericentrin (PCNT), a coiled-coil protein that can bind to the mother centriole through its C-terminal PACT (pericentrin-AKAP450 centrosomal targeting) domain and form fibrils which extend to the periphery of the PCM (Delaval and Doxsey, 2010; Gillingham and Munro, 2000; Mennella et al., 2012). As the length of PCNT matches the depth of the PCM layer, it is possible that

this protein acts as a molecular ruler in the PCM (Lawo et al., 2012; Woodruff et al., 2014). CEP152 is also disposed in fibrils inside the PCM, but covers a different role than PCNT, as it is involved in the regulation of centriole duplication through its interaction with Plk4 and CPAP (Cizmecioglu et al., 2010; Lawo et al., 2012). Many other important PCM proteins, such as CDK5RAP2, CEP192 and NEDD1, rely on PCNT for their recruitment and for their disposition inside the PCM concentric layers (Lawo et al., 2012; Mennella et al., 2014; Woodruff et al., 2014).

Although the PCM structure has been uncovered recently, the exact dynamics around the PCM assembly are still unclear. It is however known that, in *C.elegans,* a crucial role is covered by SPD-5 (Hamill et al., 2002), as this protein has been reported to be able to form networks where PCM components are recruited (Woodruff et al., 2015); the formation of these networks is facilitated by Plk1 and Cep192, which are known factors involved in PCM assembly. CPAP has also been connected to PCM recruitment (Avidor-Reiss and Gopalakrishnan, 2013).

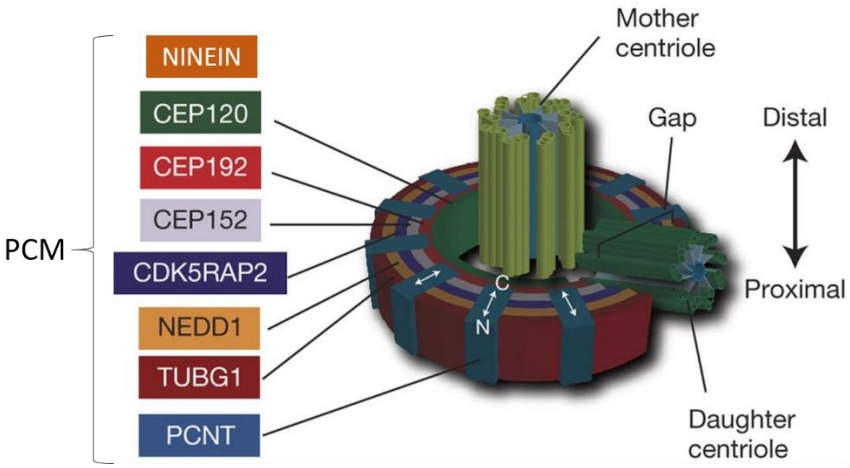

Figure 1. Schematic representation of the centrosome.
The centrosome is composed of a pair of orthogonal centrioles, named "mother" centriole and "daughter" centriole, surrounded by the protein-enriched pericentriolar material (PCM). The hierarchical disposition of the PCM proteins leads to the formation of a highly organized structure (modified from Lawo et al., 2012).

2.2.3 The Centrosome through the Cell Cycle

The centrosome's function is tightly connected to the different phases of the cell cycle. During the S-phase, to provide the cell the poles of the mitotic spindle, the centrosome undergoes duplication (Nigg and Stearns, 2011). For this event to happen, both the centrioles are required to "nucleate" a new daughter centriole, which remains associated to his mother (Conduit et al., 2015); at this stage, PCM is still concentrated around the mother centriole. While progressing to G2-M phase, the two centrosomes start to move away from each other, and the fibrous material that connects the parental centrioles (the "linker") during interphase breaks (Conduit et al., 2015). At the same time, PCNT and other PCM proteins become the substrate of the Plk1 kinase (Lee and Rhee, 2011). Through this reaction, the PCM temporarily expands, assumes a gel-like appearance and recruits additional PCM proteins that enhance the nucleating ability of the centrosome; the increased microtubule density helps to assemble the mitotic spindle (Lee and Rhee, 2011; Fry et al., 2017). Other centrosomal kinases, such as Aurora A, are implicated in this PCM maturation process (Asteriti et al., 2015). After mitosis, the cell divides in between the poles, making sure that the newborn cells contain only one centrosome (Conduit et al., 2015). The inactivation of Plk1 and dephosphorylation events on the PCM proteins, finally, results in the return of PCM to its normal composition (Fry et al., 2017).

2.3 Microtubule Nucleation and Anchoring

At the centrosome, the main function of the PCM proteins is the regulation of microtubule nucleation, anchoring and stabilization (Figure 2; Paz and Lüders, 2018). Surprisingly, many studies have proven that the presence of centrioles is not necessary for these processes: for example, flies depleted of centrioles do not dye because of microtubules-related defects, but because of the lack of cilia (Basto et al., 2006). Therefore, the activity of the PCM proteins is crucial for the control of microtubule arrays in time and space.

2.3.1 Microtubule Nucleation

Microtubules form from the association of asymmetric αβ-tubulin dimers (Tovey and Conduit, 2018). After the resulting protofilaments have been assembled into tubes, two different types of ends can be observed: the fast-growing plus end, which is responsible for interaction with different organelles and vesicles, and the slow-growing minus-end, which is usually maintained anchored in order to arrange a particular microtubule pattern (Akhmanova and Steinmetz, 2015; Martin and Akhmanova, 2018; Nogales and Wang, 2006).

The reaction that leads to the formation of microtubules is, however, highly kinetically unfavorable, and therefore requires the presence of a macromolecular template to accelerate the process : this role is covered by the γ-tubulin ring complex (γ-TuRC), considered the principal nucleator of microtubules in animal cells (Sulimenko et al., 2017; Teixidó-Travesa et al., 2012; Zheng et al., 1995). The basic unit of γ-TuRC is a heterotetramer (called γ-TuSC) containing two molecules of γ-tubulin, one molecule of GCP2 and one molecule of GCP3 (Gunawardane et al., 2000; Murphy et al., 1998); multiple γ-TuSCs can assemble with GCP4, GCP5, and GCP6 to produce γ-TuRC (Guillet et al., 2011; Kollman et al., 2011). Other proteins can also participate in the γ-TuRC complex to regulate its localization and activity: the first of these proteins, NEDD1 (Grip71 in *Drosophila* (Gunawardane et al., 2000)), can interact with γ-TuRC via its C-terminal region and can recruit γ-TuRC to different MTOCs, but seems to not participate in the assembly of the complex (Manning et al., 2010; Tovey and Conduit, 2018). The second molecule, MOZART1 (MZT1), can directly interact with the N-terminal domains of the GCP proteins and might serve as an adaptor for the interaction between NEDD1 and the ring complex (Dhani et al., 2013; Tovey and Conduit, 2018). It remains to be clarified whether MZT1 is also involved in the γ-TuRC assembly (Cota et al., 2017; Lin et al., 2016).

Although in higher eukaryotes the assembly of γ-TuRC takes place in the cytosol, the nucleating complex can only be efficiently functional if recruited to a MTOCs and activated therein (Tovey and Conduit, 2018). Many PCM proteins play a role in this process, by recruiting and activating γ-TuRC and by ensuring the effectiveness of the microtubule network formation (Tovey and Conduit, 2018). CDK5RAP2, Myomegalin, PCNT and NEDD1 represent some of the factors that can induce the recruitment of γ-TuRC (Choi et al., 2010; Haren et al., 2006; Roubin et al., 2013; Takahashi et al., 2002). Interestingly, most of these proteins (with NEDD1 being an important exception) are large and rich in coiled-coil domains (Paz and Lüders, 2018). Moreover, some share a 60-amminoacid-long N-terminal domain, called centrosomin motif 1 (CM1 (Lin et al., 2014; Sawin et al., 2004)), that is necessary for the interaction with γ-TuRC and is involved in its activation (Choi et al., 2010; Lynch et al., 2014; Tovey and Conduit, 2018). In the next subchapter (2.3.1.1-4), a brief summary about the characteristics of these proteins is provided.

2.3.1.1 CDK5RAP2

CDK5 regulatory subunit-associated protein 2 (CDK5RAP2) is a PCM protein that plays an important role in the organization of microtubules at the centrosome, especially by ensuring the association between γ-TuRC and the centrosome and by regulating centrosome cohesion (Fong et al., 2008; Graser et al., 2007a). While its depletion can cause disorganized microtubules and defective mitotic spindles

(Fong et al., 2008), mutations in its gene have been associated with the autosomal recessive primary microcephaly (MCPH), a neurodevelopmental disorder where neuronal progenitors undergo premature differentiation (Buchman et al., 2010).

Importantly, CDK5RAP2 has been described not only as a γ-TuRC recruiting factor, but also as a powerful activator of γ-TuRC-dependent nucleation in *in vitro* experiments (Choi et al., 2010). The interaction with γ-TuRC involves its CM1 domain, whereas the centrosomin motif 2 (CM2) domain, located at the C-terminal, is essential for the centrosomal association with AKAP9 and PCNT, which acts as its recruitment factor (Buchman et al., 2010; Choi et al., 2010; Sawin et al., 2004; Wang et al., 2010).

2.3.1.2 Pericentrin

Pericentrin is an elongated protein involved in the assembly of the structure of PCM, in the formation of cilia and in the organization of the mitotic spindle, where its interaction with GCP2 and GCP3 is required to stabilize γ-tubulin complexes at the spindle poles (Jurczyk et al., 2004; Mennella et al., 2012; Zimmerman et al., 2004). Similarly to CDK5RAP2, mutations of its gene have been connected to the microcephalic osteodysplastic primordial dwarfism type II (MOPD II), whose phenotype include microcephaly and post-natal growth retardation (Majewski et al., 1982; Rauch et al., 2008). The centrosomal recruitment of PCNT, although not completely understood, is mediated by its calmodulin-interacting PACT domain, located in the C-terminal region (Gillingham and Munro, 2000); the N-terminal domain, on the other end, has been described as fundamental for the recruitment of γ-TuRC at the centrosome (Takahashi et al., 2002).

2.3.1.3 AKAP9

AKAP9 (also known as AKAP450) is a giant PCM protein that shares many characteristics with PCNT. In fact, it forms coiled-coil domains for the majority of its length, (Gillingham and Munro, 2000), it localizes to the centrosome trough a PACT domain at the C-terminal, and it can associate with calmodulin, CDK5RAP2, and γ-TuRC (Gillingham and Munro, 2000; Takahashi et al., 2002; Wang et al., 2010). Possibly, AKAP9 and PCNT bind to the same location at the centrosome, as it has been shown that overexpression of this proteins leads to a dramatic decrease of PCNT signal at the centrosome (Gillingham and Munro, 2000). The role covered by AKAP9 at the centrosome is less crucial than other PCM proteins; however, it is fundamental for the organization of microtubules at another MTOC, the Golgi apparatus ((Rivero et al., 2009), see chapter 2.4).

2.3.1.4 NEDD1

NEDD1 is a PCM component whose structure is unrelated from the one of the other PCM proteins (Haren et al., 2006; Lüders et al., 2006). Its roles at the centrosome, where it is recruited via the interaction with its partner CEP192, include the organization of microtubule arrays, for example by targeting γ-TuRC at the centrosome through its C-terminal domain, and the duplication of centrioles (Gomez-Ferreria et al., 2012; Haren et al., 2006; Lüders et al., 2006; Pinyol et al., 2013; Walia et al., 2014). During mitosis, NEDD1 is needed to recruit γ-TuRC along the spindle, and its depletion is associated with defective mitotic spindles (Haren et al., 2006; Lüders et al., 2006; Scrofani et al., 2015).

As in keratinocytes different phenotypes have been found for the depletion of NEDD1 and CDK5RAP2 (defects in microtubules anchoring for the first, decreased nucleation for the second), the presence of two different γ-TuRC pools has been proposed (Muroyama et al., 2016). In this model, the γ-TuRC-NEDD1 complex would act primarily in anchoring of microtubules, whereas nucleation would be regulated by the γ-TuRC-CDK5RAP2 complex. Many studies have also demonstrated that NEDD1, in opposition to the CM1-domain-containing PCM proteins, can be purified together with γ-TuRC (Gunawardane et al., 2000, 2003; Hutchins et al., 2010; Murphy et al., 2001). This suggests that the interaction between NEDD1 and γ-TuRC can be established already in the cytosol, and that the formation of this complex could act to interfere the binding of γ-TuRC by the CM1-proteins in order

to avoid the activation of γ-TuRC before it is recruited to a MTOC site (Tovey and Conduit, 2018). Despite the high number of studies about NEDD1, it is clear that its role remains to be clarified, especially in relation to the nucleation and anchoring activity.

2.3.2 γ-TuRC-Independent Nucleation

Surprisingly, it has been shown that microtubule nucleation can still take place even in the absence of γ-tubulin (albeit at a lower rate) (Hannak et al., 2002; Lüders et al., 2006; Strome et al., 2001). As a consequence, it is possible that other proteins act inside the cell in order to ensure a backup mechanism in the case of γ-tubulin loss. Tog domain-containing proteins, such as XMAP215/chTOG, and the homologues of TPX2 represent good candidates, as it is already known that they can stimulate γ-TuRC-dependent nucleation and microtubule stability (Flor-Parra et al., 2018; Roostalu et al., 2015; Thawani et al., 2018; Wieczorek et al., 2015; Woodruff et al., 2017). XMAP215/chTOG are microtubule polymerases able to use their Tog domain to interact with tubulin dimers. By doing that, they can facilitate the polymerization of tubulin dimers at the plus end and stimulate microtubule growth (Flor-Parra et al., 2018; Roostalu et al., 2015; Thawani et al., 2018). The spindle assembly factor TPX2, on the other hand, promotes nucleation by activating Aurora A, the kinase responsible for the phosphorylation of NEDD1, and by acting as a stabilizing and anti-catastrophe factor on microtubule intermediates and newly made microtubules (Reid et al., 2016; Roostalu et al., 2015; Wieczorek et al., 2015; Woodruff et al., 2017). Several *in vitro* studies have proven that these two proteins are able to nucleate microtubule independently, without the need of the template γ-TuRC or high tubulin concentrations (Roostalu et al., 2015; Woodruff et al., 2017). Nevertheless, the interaction between γ-tubulin, TPX2 and chTOG has also been demonstrated, suggesting that these proteins might act in synergy with γ-TuRC to ensure robust nucleation (Paz and Lüders, 2018; Tovey and Conduit, 2018).

2.3.3 Microtubule Anchoring

After being nucleated, microtubules can remain associated at the centrosome, where they are arranged to form the typical aster, or move to alternative cellular locations, where they similarly contribute to the formation of different kinds of patterns. Either way, in order to maintain their disposition, microtubules need to be attached (that is, anchored) to a scaffolding surface (Martin and Akhmanova, 2018). Although the exact mechanism by which this process happens is not completely clear yet, it is thought that the cell relies on the ability of the nucleator γ-TuRC to bind to minus ends and act as a stabilizing factor in order to anchor microtubules (Anders and Sawin, 2011; Moritz et al., 1995; Wiese and Zheng, 2000; Zheng et al., 1995). Nevertheless, the presence of additional proteins seems also to be essential for this process to be successful: Ninein, resident on the distal appendages of the mother centriole, has been proposed as a key player in this system ((Delgehyr et al., 2005; Mogensen et al., 2000), see chapter 2.5). Other examples include the CAMSAP proteins, which can associate to uncapped microtubules minus ends and thus stabilize them, and NEDD1, which has recently been proposed as an anchoring factor for its ability of targeting minus-ends to non centrosomal locations (Jiang et al., 2014; Muroyama et al., 2016). Trichoplein, PCM1, CEP135, ODF2, EB1 and MSD1/SSX2IP seem also to be involved in microtubule anchoring, together with the minus-end directed motor dynein (Askham et al., 2002; Dammermann and Merdes, 2002; Ibi et al., 2011; Nakagawa et al., 2001; Ohta et al., 2002; Quintyne et al., 1999; Young et al., 2000). Dynein covers a central role in anchoring of microtubules, as many of the proteins involved in this process, such as ninein and MSD1/SSX2IP, depend on its transport (Dammermann and Merdes, 2002; Hori et al., 2014; Redwine et al., 2017). In this way a positive feedback loop, with dynein delivering anchoring factors at the centrosome through microtubules, can be established.

Many of the proteins that are thought to be involved in anchoring of microtubules reside on the mother centriole's subdistal appendages, but surprisingly the lack of these structures doesn't totally impair nucleation and anchoring (Ishikawa et al., 2005); for this reason, it is still not clear if the

PCM could represent an anchoring site for microtubules. Similarly, it remains to be established whether γ-TuRC is always required for minus-end capping at the centrosome and what is the exact mechanism through which some anchoring factors act.

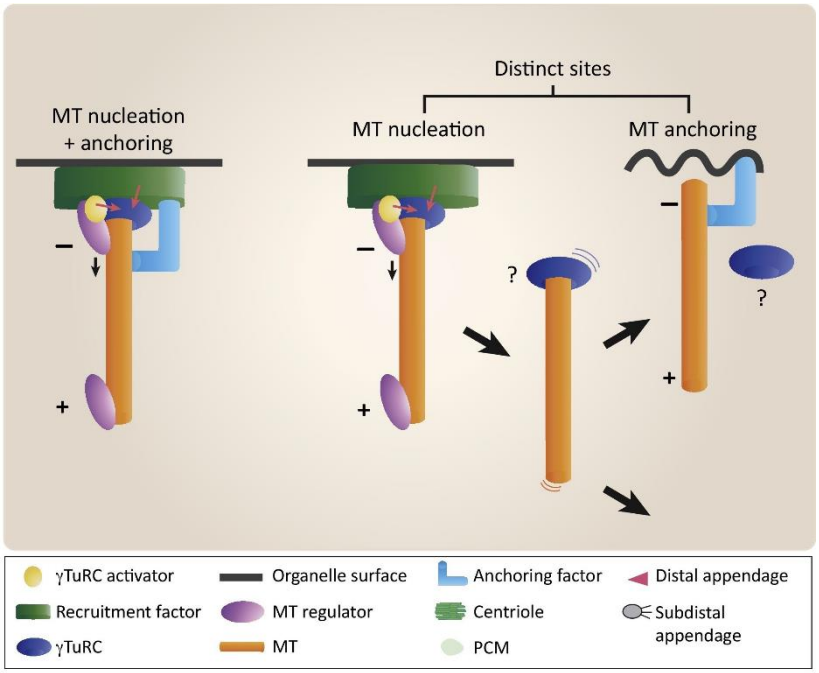

Figure 2. Schematic representation of microtubule nucleation and anchoring processes at the centrosome.

Microtubules can be nucleated and anchored at the same location or be transferred to form patterns at a different site. Nucleation requires the presence of the nucleator γ-TuRC, recruited by specific PCM factors; other proteins might also participate in nucleation, by activating γ-TuRC or by regulating plus-end or minus-end dynamics. In the case of anchoring, it is unknown whether γ-TuRC is necessary, and how the transport of microtubules towards the anchoring site is managed. (from Paz and Luders, 2018).

2.4 Microtubule Organization at the Golgi Apparatus

Despite being the major site for nucleation and anchoring in animal cells, the centrosome is not the only cellular location where microtubules can be organized to form a network. In fact, even in cells where a well-defined radial microtubule array can be distinguished, other MTOCs can provide alternative attachment sites. Among those sites are the nuclear envelope, the cell cortex and the Golgi Apparatus, which constitutes the second most important MTOCs in mammals (Chabin-Brion et al., 2001; Masoud et al., 2013; Nogales and Wang, 2006). The microtubule-organizing activity of the Golgi can be so prominent that, in some cell lines, such as retinal pigmented epithelium (RPE) cells, almost 50% of the entire microtubule population are nucleated in this cellular compartment (Efimov et al., 2007). Differently from the centrosomal-assembled arrays, microtubules at the Golgi are organized in a polarized fashion that regulates cell asymmetry and serves as an highway to carry cargos to the periphery (Hurtado et al., 2011; Vinogradova et al., 2009, 2012).

Many of the PCM proteins that regulate microtubule organization at the centrosome are also found at the Golgi apparatus, where their dynamics are often different (Figure 3). The organization of the microtubule network at this compartment, in fact, depends on a protein that represents a minor player at the centrosome: AKAP9. AKAP9's ability to reach the cis-Golgi surface depends on its N-terminal domain, which recognizes the Golgi-resident factor GM130 (Hurtado et al., 2011; Rivero et al., 2009). From this location, it can stimulate the formation of new microtubules by recruiting γ-TuRC and by promoting the accumulation of CDK5RAP2 and its paralog myomegalin, which in turn are also

able to increase the amount of γ-TuRC at the cis-Golgi surface (Roubin et al., 2013; Wang et al., 2010, 2014; Wu et al., 2016). Despite CDK5RAP2 being the most powerful nucleator among these proteins, it has been demonstrated that only AKAP9 is essential for microtubule nucleation, whereas CDK5RAP2 and myomegalin can only enhance this activity; in AKAP9-depleted RPE cells, in fact, nucleation at the Golgi is abrogated (Wu et al., 2016).

However, microtubules nucleated at the Golgi need additional factors in order to be stabilized and anchored on this site: the first is CAMSAP2, which localizes at the Golgi by interacting with both AKAP9 and myomegalin (Wu et al., 2016). CAMSAP2 has other two homologues in mammals (CAMSAP1 and 3) and can stabilize growing microtubules devoid of their γ-TuRC cap by associating to their minus ends; when depleted, the microtubules nucleated outside the centrosome can no longer be observed (Jiang et al., 2014; Nogales and Wang, 2006). Similarly to CAMSAP2, two members of the End Binding (EB) proteins family, EB1 and EB3, are involved in interactions with myomegalin and interact with plus and minus ends of microtubules (Roubin et al., 2013; Wang et al., 2014). In cells lacking myomegalin or EB1/3, CAMSAP2-enriched microtubules are not able to associate to the Golgi surface (Tanaka et al., 2012). Finally, microtubules stabilized by CAMSAP2 require the presence of the plus-end binding proteins CLASP1 and CLASP2 (Wu et al., 2016; Efimov et al., 2007). These factors can regulate the association of microtubules to the *trans*-Golgi surface by interacting with GCC185 (Efimov et al., 2007), and, most importantly, can promote the nucleation activity by making more kinetically favorable the otherwise slow template-dependent microtubule growth (Sanders and Kaverina, 2015).

Interestingly, the relation between the centrosome-based microtubules and the Golgi-derived network seems to be based on competition, as the inactivation of one of the two pathways leads to the enhancement of the other: for example, decreased levels of AKAP9, crucial for nucleation at the Golgi, results in the enhanced recruitment of γ-TuRC at the centrosome (Gavilan et al., 2017); on the other hand, the inhibition of centrosomal function causes the recruitment of several PCM components, such as PCNT and γ-TuRC, on the Golgi (Gavilan et al., 2017).

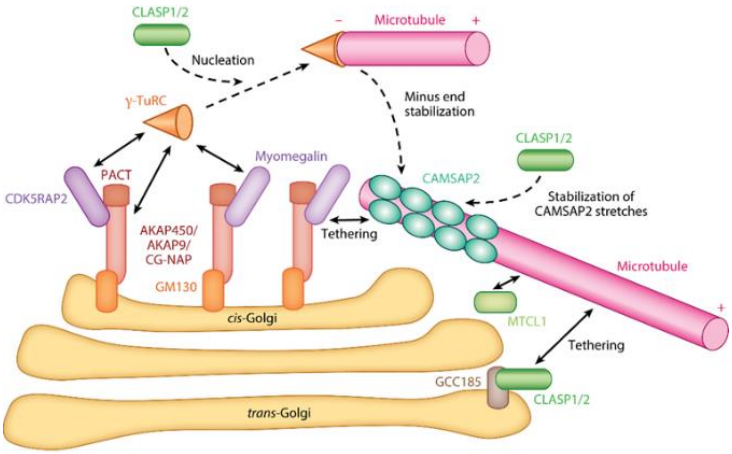

Figure 3. Schematic representation of the organization of microtubules at the Golgi apparatus.

At the cis-Golgi surface, nucleation of new microtubules is promoted by the recruitment of γ-TuRC by AKAP9, CDK5RAP2 and its paralog myomegalin. AKAP9 acts as a scaffold to recruit CDK5RAP2 and myomegalin through its PACT domain, and its localization at this compartment depends on its interaction with the Golgi marker GM130. Pre-existing microtubules that have lost their γ-TuRC cap are stabilized by the association of CAMSAP2 to their minus ends and are anchored at the Golgi through the interaction with the AKAP9/myomegalin complex. CLASP2 and 1 participate in microtubules stabilization, promote the tethering of microtubules at the trans-Golgi network via the interaction with GCC185 and stimulate γ-TuRC-dependent nucleation (from Wu and Akhmanova, 2017).

2.5 The Role of Ninein in Microtubule Organization

One of the most important factors needed at the centrosome to ensure the stable anchoring of microtubules is Ninein. Ninein is a 245 kDa coiled-coil rich protein which localizes to the subdistal appendages of the mother centriole, containing four leucine zipper motifs in the central region, a GTP binding site as well as a EF-hand-like domain in the N-terminal domain (Bouckson-Castaing et al., 1996; Mogensen et al., 2000). The functions covered by Ninein at the centrosome are not only related to microtubule anchoring and include centrosome cohesion, mitotic regulation and ciliogenesis (Chen et al., 2003; Graser et al., 2007b; Mazo et al., 2016). Moreover, Ninein is found in several cell types, including epithelial cells, neurons and muscle cells, where it is involved in the regulation of the formation of non-centrosomal microtubule arrays (Bugnard et al., 2005; Sumigray and Lechler, 2011; Zhang et al., 2016). Importantly, mutations in the Ninein gene have been associated with a rare primordial dwarfism disorder, called Seckel syndrome, characterized by impaired cognitive abilities, microcephaly and order defects (Dauber et al., 2012).

Despite the importance of the role covered by Ninein in microtubule anchoring, it is currently not known how this protein fulfills its functions. Whether Ninein is able to anchor microtubule by directly binding to their minus-ends, for example, is not clear. Most importantly, however, it remains to be clarified whether Ninein acts only in microtubule anchoring and release, or if it is also involved in the regulation of microtubule nucleation, as proposed by several studies (Delgehyr et al., 2005; Lin et al., 2006; Stillwell et al., 2004). These questions led us to investigate more into detail the role of Ninein in the regulation of microtubule organization, focusing in particular on the processes of microtubule anchoring and nucleation. Furthermore, we decided to characterize the interaction between Ninein and CLASP2, a centrosomal protein which we observed was displaced from the centrosome in the absence of Ninein.

3. Materials and Methods

3.1 Cell Culture

The RPE 4KO (AKAP9 $^{-/-}$, MMG $^{-/-}$, CDK5RAP2 $^{-/-}$, CAMSAP2 $^{-/-}$) cell line used for this project was established by former PhD student Jingchao Wu. RPE cell lines, HeLa cells and HEK 293T cells were cultured in 100 mm x 20 mm Petri dishes in Full Medium (1:1 mixture of Dulbecco's Modified Eagle Medium (DMEM, Sigma-Aldrich) and F-10 medium (Lonza) with 10% Fetal Bovine Serum (FBS, GE Healthcare)) and kept in a humidified incubator at 37°C and 5% CO_2 concentration to guarantee the ideal growth conditions. Approximately every four days, when the maximal cell confluence was reached, cells were splitted using the following procedure: the old medium was removed from the dish, 10 ml of Phosphate Saline Buffer (PBS, Sigma-Aldrich) were used to wash the cells and remove all the traces of medium, and 1 ml of 0.05 Trypsin EDTA (Gibco, Life Technologies) was added to the cells in order to detach them from the dish surface. After incubating the dishes again in the incubator at 37°C and 5% CO_2 concentration for several minutes in order for the Trypsin to act efficiently, 1 ml of fresh full medium was added to the cells to neutralize the effect of Trypsin. The appropriate volume of cells was then transferred in a new Petri dish with fresh Full Medium to obtain the desired confluence.

3.2 Generation of RPE NIN KO Cell Line

RPE NIN KO cell line was generated by using the CRISPR/CAS9 genome editing technology. For this, RPE WT cells were grown until the proper confluence was reached (≈ 20-50%) and transfected with the plasmid px459-NIN-sgRNA4 (sequence: GGCCGCGCTTCTTCATCCAG) on day 0. Cells were given a day (day 1) to recover and grow. On day 2, the successfully transfected cells were selected by adding to the cells puromycin-containing full medium at 20 µg/ml. The drug treatment was repeated for another day before cells were given medium without puromycin for 2 days in order for them to recover and grow. A small percentage of cells was then used for immunofluorescence staining to verify the success of the knock-out procedure. After this step, cells were diluted and plated in 96 well plates in order to obtain single-cell populations. Single colonies were grown for 7-10 days and stained again to select knock out populations. Finally, in order to prove the efficiency of the knockout procedure, immunofluorescence staining, Western Blot and sequencing of Ninein gene were performed (Figure S2).

3.3 Molecular Cloning

3.3.1 PCR

Every PCR reaction was prepared on ice by mixing 38 µl of milliQ water, 10 µl Phusion High Fidelity 5X buffer (Thermo Scientific), 0.5 µl of 25 mM dNTPs, 0.5 µl of primers forward and reverse (listed in Table S1), 1 µl of DNA template (at the concentration 50 ng/ µl) and finally 0.5 µl of Phusion Polymerase enzyme (Thermo Scientific). The final solution of 50 µl was divided in two PCR tubes and placed in the TProfessional Basic PCR Thermocycler (Biometra) where the PCR reaction was performed. The cycles used, together with temperatures and durations, are listed in Table 1 below.

Step	Temperature	Duration
Denaturation	98 °C	30 s
Denaturation x 30	98 °C	10s
Annealing	59 °C	30 s
Extension	72 °C	1 min
Final Extension	72 °C	10 min
Cooling	20°C	10 min

Table 1. Steps, Temperatures and Durations of a typical PCR program.

3.3.2 Isothermal Cloning

PCR was employed to generate both Ninein and CLASP2 truncations (listed in Table S2). For Ninein and CLASP2 truncations, Bio-Tev mCherry NIN 601-1050, Bio-Tev mCherry NIN 1401-2090 and StrepII-mCherry-CLASP2 FL were used as PCR templates. The Gibson Assembley Master Mix (Clontech Laboratories) was subsequently used to insert the obtained PCR products into the empty vectors pEGFP-C1 and pBtm-C1. The empty vectors have been obtained by digesting the already existing constructs Bio-Tev mCherry NIN 601-1050 and pEGFP-C1-NIN 601-1050 with the Fast Digest restriction enzymes BglII and EcoRI (Thermo Fisher). The digestion reaction was prepared as Table 2 describes and incubated for 30 minutes at 37°C to allow the enzymatic digestion to happen.

Reaction Component	Amount
plasmid	4 µg (4 µl)
10X Fast Digest Green Buffer (Thermo Fisher)	4 µl
Fast Digest BglII	3 µl
Fast Digest EcoRI	3 µl
milliQ H_2O	26 µl

Table 2. Digestion reaction used to obtain the empty vectors from Bio-Tev mCherry NIN 601-1050 and pEGFP-C1-NIN 601-1050.

After incubation, the digested constructs were run on a 1% Agarose gel in TAE buffer (40 mM Tris, 20mM acetic acid and 1 mM EDTA) for 20 minutes at 120V together with GeneRuler 1kb DNA Ladder (Thermo Fisher). The empty vectors were then extracted from the agarose gel and purified by using the Wizard PCR Preps DNA Purification System (Promega) following the manufacturer instructions. The obtained DNA was finally used together with the PCR products to generate the constructs listed in Table S2.

3.3.3 Bacterial Transformation

To transform the competent bacteria E. coli DH10, 2 µl of each Gibson Assembly product were added to 50 µl of competent bacteria on ice. These were incubated on ice for 30 minutes, placed in a warm bath at 42 °C for 30 seconds to allow heat shock to happen and subsequentially placed in ice again for 2 minutes. 950 µl of room temperature Luria-Bertani (LB) medium without antibiotic (0.05% yeast extract, 1% w/v tryptone, 0.05 g/L NaCl in ddH_2O) were then added to each tube. The transformed bacteria were incubated at 37°C for one hour in a shaking incubator, spreaded on antibiotic positive LB-agar medium (5 g/L yeast extract, 10 g/L tryptone, 10 g/L NaCl in deionized water, pH 7.0, 15 g/L agar) in Petri dishes and incubated over night at 37°C in a bacterial incubator. The next day, single

colonies were picked and grown in 10 ml of antibiotic positive LB medium over night at 37°C in a shaking incubator.

3.3.4 DNA Plasmid Verification by Restriction Profile

The plasmids grown over night in 10 ml of LB medium were purified by using the PureLink® Quick Plasmid Miniprep Kit (Thermo Fisher). To verify the success of the cloning procedure, 1 µg of each purified construct was digested for 30 minutes at 37°C with 0.5 µl of the appropriate Fast Digest Restriction Enzyme (Thermo Fisher), 2 µl of 10X Fast Digest Green Buffer (Thermo Fisher) and milliQ H_2O in a final reaction of 20 µl. The constructs were run on a 1% Agarose gel in TAE buffer (40 mM Tris, 20mM acetic acid and 1 mM EDTA) for 20 minutes at 120V together with GeneRuler 1kb DNA Ladder (Thermo Fisher). Finally, clones of the expected size were isolated and sequences to verify the result of the restriction profile analysis.

3.4 **Knock Down via RNA Interference**

To investigate the role of Ninein in the processes of microtubule anchoring and nucleation, depletion of the protein via RNA interference was employed. For this, RPE 4KO cells were seeded in 2 cm wells and cultured until the appropriate confluence (≈ 40%) was reached. The cells were then transfected with the Ninein siRNA by performing the following steps: first, old medium was removed and replaced by fresh warm medium. Then, two mixes of 100 µl each were prepared: solution A containing 2 µl of 20 µM siRNA (sequence: CGGUACAAUGAGUGUAGAATT) and 100 µl OPTIMEM medium (Thermo Fisher), and solution B containing 6 µl of the transfectant agent (Lipofectamine™ RNAiMAX Transfection Reagent®, ThermoFisher) and 100 µl of OPTIMEM medium. Both solutions were gently vortexed nine times before solution B was added to solution A. The resulting mix of 200 µl was lightly vortexed nine times and incubated at room temperature for 10 minutes. Finally, the solution was added drop wise to the cells. 24 hours after the transfection occurred, old medium was replaced with fresh warm medium. The cells were then used for two different purposes: to investigate how the protein affects microtubule anchoring at the centrosome and to study the role of Ninein in microtubule nucleation (see the following chapter, 3.5). In the first case, 48 hours after siRNA transfection, RPE 4KO cells depleted of Ninein and control cells (RPE 4KO) were treated with Tymidine 5 mM in order to block the cell cycle and compare microtubule density in the two different conditions. 72 hours after siRNA transfection, depleted and control cells were fixed and stained for α-tubulin, Ninein and PCNT as described in chapter 3.7.

3.5 **Nocodazole Washout Assay**

To explore the role of Ninein in microtubule nucleation, RPE 4KO cells depleted of Ninein were used to perform a nocodazole washout assay. In particular, 48 hours after transfection RPE 4KO cells depleted of Ninein were mixed with control cells (RPE 4KO) and plated in 24-well plates with cover slips in order to reach 60% confluence in the following day. In the following day (between 48 and 72 hours after transfection), cells were used to perform the washout experiment.

For this, cells were incubated on ice at 4°C for 1 hour in cold full medium containing 10 µM Nocodazole, a drug able to depolymerize microtubules. Subsequently, cells were washed 6 times with cold medium in order to remove every trace of Nocodazole. The well plates were then placed in a warm bath at 37°C and the cells were immediately added fresh warm medium (without Nocodazole) in order for microtubule regrowth to take place. After 30 seconds, 1 minute, 1.5 minutes or 2 minutes of incubation in the warm bath, cells were fixed and processed as explained in 3.7 for immunofluorescence staining. In particular, to visualize the microtubule regrowth process, cells were stained for the plus-end tracking protein EB1, for Ninein and for PCNT.

3.6 **Relocation Assay**

RPE 2 KO were seeded in a 24 well plate in order to achieve 60% confluence in 24h. They were then transfected with the plasmid pEGFP-AKAP9 1-1029^NIN FL by performing the following steps: solution A, containing 25 µl of OPTIMEM medium and 500 ng of pEGFP-AKAP9 1-1029^NIN FL, and solution B, containing 25 µl of OPTIMEM medium and 1.5 µl of FuGENE® transfection reagent (Promega), were prepared and lightly vortexed 9 times. Solution B was the added to solution A; the obtained mix was lightly vortexed 9 times, incubated for 15 minutes at room temperature and finally added drop by drop to the cells. 24 hours later, the cells were fixed and stained by following the protocol described in section 3.7. In particular, cells were stained for γ-tubulin and GM130.

3.7 **Immunofluorescence Staining**

Cells were fixed by removing the old medium and adding ice-cold 100% Methanol to the wells. Cells were incubated at -20°C for five minutes and methanol was quickly removed and completely washed away by adding 1X PBS to the wells. Cells were incubated at room temperature on a shaker for five minutes, PBS was removed and PBST (1X PBS + 0.1% Triton X-100) was added to the cells in order to form holes in the cells' plasma membranes. The wells were incubated for two minutes at room temperature on a shaker and subsequently washed with PBST (1X PBS + 0.05% Tween-20) for three times for five minutes at room temperature. Filtered 2% BSA (diluted in PBST) was then used to block the cells for twenty minutes at room temperature. Next, the coverslips were transferred from the wells to a wet box, and incubated with the primary antibody diluted in blocking buffer (Table 3) for one hour at room temperature. Excess of primary antibody was removed by washing the coverslips thrice with 1X PBST for five minutes at room temperature, and cells were subsequently incubated with secondary antibody diluted in 1X PBST for one hour at room temperature. 1X PBST was again used to remove any excess of secondary antibody by washing the cells thrice for five minutes. Finally, coverslips were transferred from the wet box to tissue paper, where they were washed with 96% Ethanol to dry them out. After ten minutes, when the coverslips resulted completely dry, they were transferred on glass slides using 4', 6-Diamidino-2-Phenylindole (DAPI)-containing Vectashield mounting agent (Vector Laboratories, CA, USA). Cells were imaged on a Nikon DS-Qi2 upright microscope with CFI Plan Fluor 100X oil objective (Nikon). ImageJ software, MetaMorph software and GraphPad software were employed to modify and analyze the images.

Target Protein	Species of Origin	Dilution Used	Company
NInein (NIN)	Mouse	1/200	Santa Cruz Biotechnology
Ninein (NIN)	Rabbit	1/300	Bethyl
Pericentrin (PCNT)	Mouse	1/500	Abcam
Pericentrin (PCNT)	Rabbit	1/600	Abcam
NEDD1	Mouse	1/300	Abnova
CLASP2	Rabbit	1/400	Homemade
γ-tubulin	Rabbit	1/500	Sigma
GM130	Rabbit	1/800	BD Biosciences
EB1	Rat	1/200	Homemade
α-tubulin	Rat	1/300	Pierce

Table 3. Primary antibodies used for Immunofluorescence staining.

3.8 Pull Down Assay

Pull down assay was employed to demonstrate the interaction between Ninein and CLASP2 and to map the domains responsible for this interaction. The constructs used in this experiment are listed in Table S3, together with their characteristics.

To this end, HEK 293T cells were seeded in 2 cm wells and cultured until the appropriate confluence for transfection (≈ 60%) was obtained. Prior to transfection, the old medium was removed from the wells and substitute with fresh warm medium. For transfection, two mixes of 100 µl were prepared for each well: mix A containing 100 µl OPTIMEM medium (Thermo Fisher), 1 µg of pET21a-BirA, 1 µg of the prey-protein plasmid and 1 µg of the bait-protein plasmid; and mix B, containing 100 µl of OPTIMEM medium and 9 µl of PEI transfectant agent (Polysciences). Once prepared, both the mixes were lightly vortexed nine times to obtain homogeneous solutions; mix B was then added to mix A and the resulting solution was lightly vortexed nine times, incubated at room temperature for 10 minutes and finally added drop by drop to the cells. After 24 hours, the success of the transfection was verified by visualizing the fluorescence of mCherry and GFP proteins under a fluorescence microscope. Next, the old medium was removed from the wells and the cells were gently washed twice with ice-cold PBS. The cells were harvested in 1 ml of cold PBS, translocated to new Eppendorf tubes and spinned at 1000 rpm for 5 minutes at 4°C. After removing the supernatant, 100 µl of cold Lysis buffer (HEPES 50 mM pH 7.4, NaCl 150 mM, 1X Phosphatase Inhibitor, 1X Protease Inhibitor, 0.5% Triton X-100) was added to the cells, which were subsequentially incubated in ice for 10 minutes and centrifuged at 13200 rpm for 30 minutes at 4°C. 10 µl of each obtained cell lysate were isolated and kept as "input" samples. The remaining 90 µl ("pull down" samples) were incubated with Streptavidin-coated magnetic beads (Dynabeads®, Thermo Fisher), which had been previously prepared as follows: for each well, 15 µl of Dynabeads were extracted and washed two times on ice with Washing buffer (HEPES 50mM pH 7.4, NaCl 150 mM, 0.5% Triton X-100) on the Dynal magnetics separator MPC-S (Invitrogen). Next, Blocking buffer containing 0.1% chicken egg white was added to the beads. An incubation of 30 minutes in rotation at room temperature followed. The beads were then washed thrice on ice with Washing buffer to remove every trace of the blocking solution, resuspended in an appropriate volume of Washing buffer and aliquoted in new Eppendorf tubes (15 µl of beads for each tube). 90 µl of each cell lysate were added to the beads and incubated for 1 hour in rotation at 4°C to allow the biotinylated proteins to bind to the streptavidin-coated beads. After incubation, samples were placed on ice on the Dynal magnetics separator MPC-S and washed three times with 1 ml of Washing buffer. Subsequently, the "pull down" and the "input" samples were mixed with prewarmed 1X Sample Buffer (20 µl and 10 µl respectively), incubated at 100°C on a heating block for 5 minutes and then on ice for 2 minutes. The obtained samples were then used to perform a SDS-PAGE and Western Blot analysis.

3.9 SDS-PAGE and Western Blot

The samples obtained from the Pull Down experiment were analyzed using the SDS-PAGE and Western Blot techniques. First, the samples and the Precision Plus Protein ladder (Bio-Rad) were loaded on a sodium dodecyl sulfate polyacrylamide gel composed of a 5% v/v stacking region and of a running region (different percentages have been used for different gels, ranging from 6% to 8%). The samples were run in a running buffer containing glycine, Tris and 0.5% SDS at 80V for the stacking gel region and at 120V for the running gel region. After electrophoresis, the gel was washed with water and assembled in a sandwich with Extra thick Blot paper (Bio-Rad) and Amersham Protran Premium 0.45 nitrocellulose membrane (GE Healthcare). The proteins were transferred from the gel to the membrane by using the Standard SD Protocol (30 minutes, 25V) in the Trans-Blot Turbo Transfer System (Bio-Rad). Subsequently, the membrane was washed with demi water to remove every trace

of the gel and blocked for 30 minutes on a shaker at room temperature in 2% BSA diluted in PBS. Primary antibodies anti-GFP (Rabbit, Abcam, 1:4000) and anti-mCherry (Mouse, Clontech Laboratories, 1:1000), diluted in blocking buffer, where then added to the membranes and incubated over night at 4°C. Excess of antibodies was removed by washing the membranes thrice for 5 minutes with 1X PBST at room temperature. The membranes were then incubated with secondary antibodies (Goat anti Mouse 680LT and Goat anti Rabbit 800LT diluted 1:5000 in 1X PBST; Bio-Rad) for 45 minutes in rotation at room temperature, washed three times for 5 minutes with 1X PBST and scanned using the Odyssey CLx scanner (LI-COR).

4. Results

4.1 Ninein localizes at the centrosome through its C-terminal domain.

To explore the role of Ninein in microtubule organization at the centrosome, we decided to first test which of its domains mediates its localization at the centrosome. This aspect is in fact not clear yet, as conflicting results can be found in previous studies (Chen et al., 2003; Delgehyr et al., 2005; Lin et al., 2006; Stillwell et al., 2004). We therefore transfected HeLa cells with different Ninein truncations (Figure S1A and S1B) and fixed the cells after 24 hours to check the intracellular localization of the truncated proteins. Only mCherry-Ninein full length (FL) and mCherry-Ninein 601-2090 were able to localize to the centrosome, whereas all the other truncations remained diffused in the cytoplasm. As it can be argued that the recruitment of Ninein FL and Ninein 601-2090 at the centrosome is mediated by the endogenous Ninein protein in HeLa cells, we repeated the experiment in our Ninein KO RPE cell line (Figure 4A and 4B), which we previously generated through CRISPR/Cas9 genome editing technology (Figure S2). We verified the complete absence of Ninein in these cells by staining the cells with two antibodies targeting the C-terminal (Figure S2B) and N-terminal (not shown) domain of Ninein, by Western Blot (Figure S2C) and by sequencing the Ninein gene (Figure S2D). Again, in RPE NIN KO cells only the full length protein, the 601-2090 truncation and the C-terminal truncation (1401-2090 amino acidic region) of Ninein were able to localize at the centrosome. From this experiment we concluded that the C-terminal domain is responsible for Ninein's localization at the centrosome. Next, we focused on the C-terminal domain and designed other two truncations (NIN 1401-1900 and NIN 1897-2090) in order to map the minimal domain responsible for Ninein's recruitment at the centrosome; both these proteins were able to localize at the centrosome in HEK 293T cells (Figure 4C and 4D). Therefore, it can be stated that the coiled-coil domain placed at the most C-terminal region of Ninein (1897-2090 amino acidic region) is sufficient to target the protein to the centrosome.

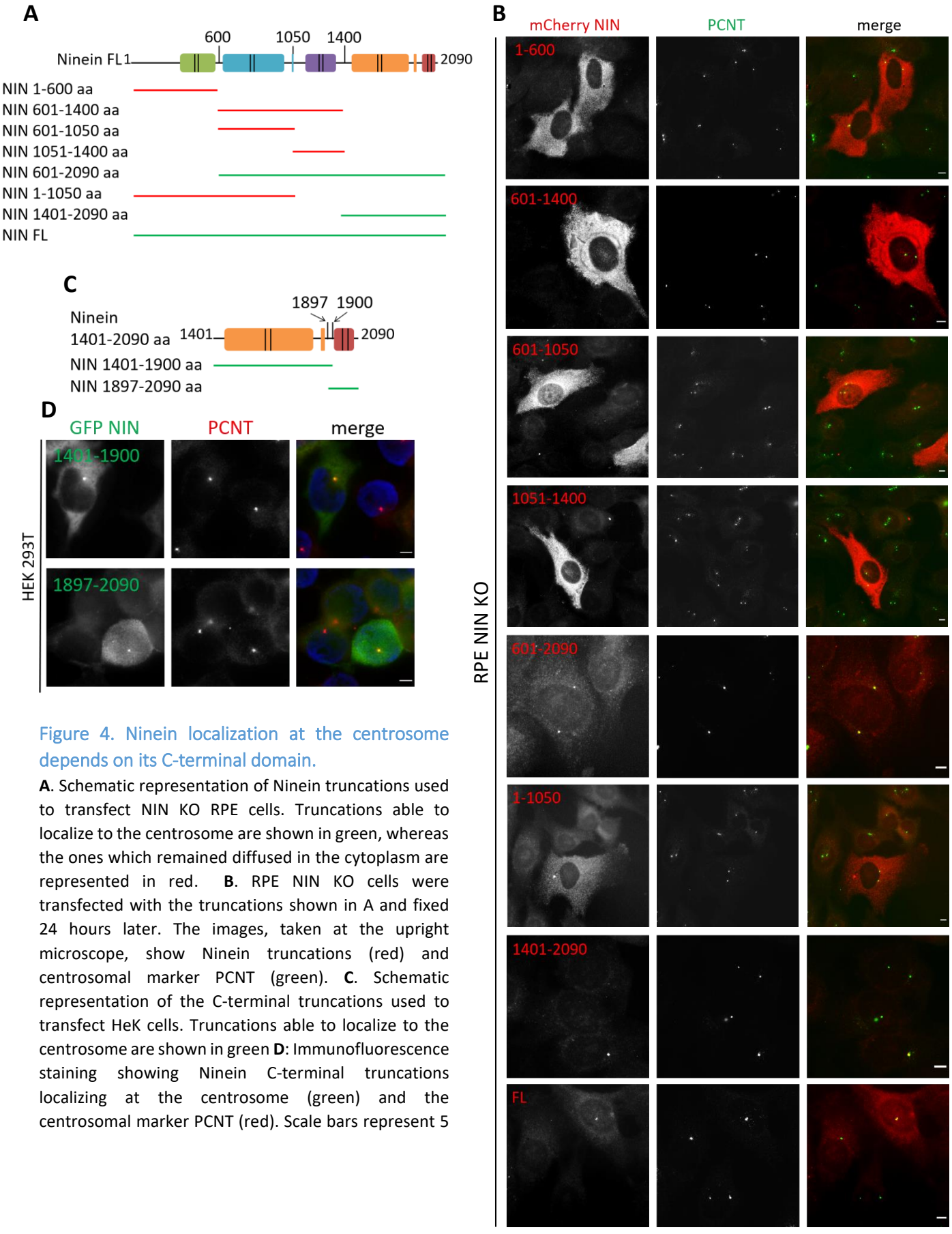

Figure 4. Ninein localization at the centrosome depends on its C-terminal domain.

A. Schematic representation of Ninein truncations used to transfect NIN KO RPE cells. Truncations able to localize to the centrosome are shown in green, whereas the ones which remained diffused in the cytoplasm are represented in red. **B**. RPE NIN KO cells were transfected with the truncations shown in A and fixed 24 hours later. The images, taken at the upright microscope, show Ninein truncations (red) and centrosomal marker PCNT (green). **C**. Schematic representation of the C-terminal truncations used to transfect HeK cells. Truncations able to localize to the centrosome are shown in green **D**: Immunofluorescence staining showing Ninein C-terminal truncations localizing at the centrosome (green) and the centrosomal marker PCNT (red). Scale bars represent 5

4.2 Microtubule density is decreased upon Ninein depletion and the normal phenotype can be rescued.

Several studies have shown that Ninein is essential for anchoring microtubules at the centrosome and that centrioles lacking Ninein are unable to successfully anchor microtubules (Delgehyr et al., 2005; Kowanda et al., 2016; Piel et al., 2000; Stillwell et al., 2004; Zheng et al., 2016). After generating our RPE NIN KO cell line, we as well observed that the normal microtubule density was impaired in these cells (Figure 5A), indeed suggesting that Ninein is involved in the anchoring process. We decided to further investigate the role of Ninein in microtubule anchoring by making use of the previously generated RPE AKAP -/-, MMG -/-, CDK5RAP2 -/-, CAMSAP2 -/- cell line (RPE 4KO). As the Golgi microtubule array is absent in these cells, this system allowed us to focus exclusively on centrosome-attached microtubules. Immunostaining of RPE 4KO cells depleted of Ninein via RNA interference strikingly revealed a dramatic decrease in microtubule density at the centrosome (Figure 5B), which we were able to rescue by transfecting the Ninein-depleted cells with GFP-Ninein FL 48 hours after siRNA treatment (Figure 5C and 5D). Taken together, these findings confirm that Ninein is involved in microtubule anchoring at the centrosome, and that its presence is needed to ensure the maintenance of a radial centrosomal microtubule array.

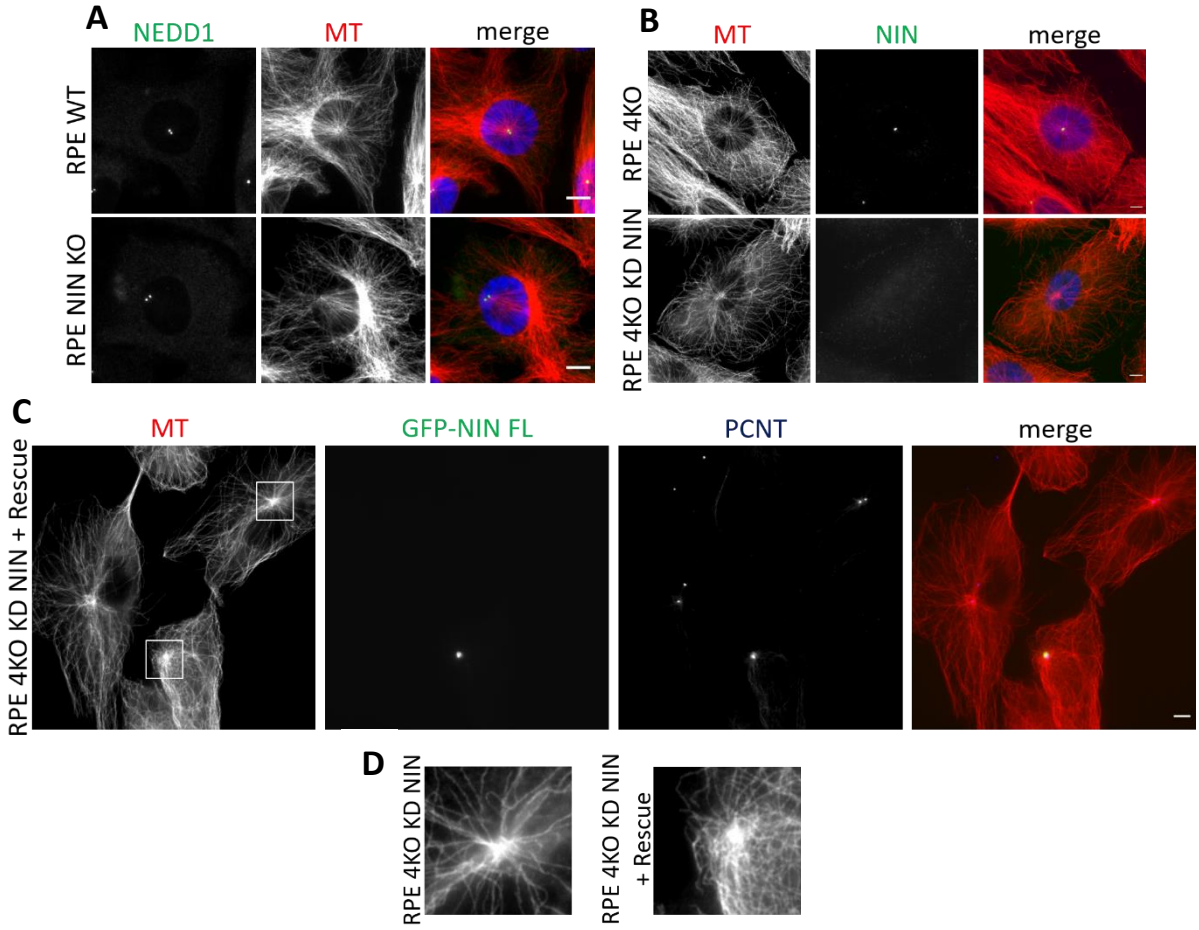

Figure 5. Ninein is involved in the anchoring of microtubules at the centrosome.

A. Immunofluorescence staining showing normal and decreased microtubule density in RPE WT and RPE NIN KO cells respectively. Cells were stained for centrosomal marker NEDD1 (green), microtubules (α-tubulin, red) and DAPI (blue). **B**. Immunofluorescence staining showing microtubule density in RPE 4KO cells and in RPE 4KO KD NIN cells. RPE 4KO cells were depleted of Ninein via RNA interference and fixed 72 hours later. Cells were stained for microtubules (α-tubulin, red), Ninein (green) and DAPI (blue). **C**: Upright microscopy images showing

microtubule density in RPE 4KO KD NIN rescued cells. RPE 4KO KD NIN cells were transfected with GFP-Ninein FL 48 hours after the depletion treatment and incubated for additional 24 hours before fixation. Cells were stained for microtubules (α-tubulin, red) and centrosomal marker PCNT (blue). **D**: Details of microtubule density in RPE 4KO KD NIN and rescued cells. Scale bars represent 5 µm.

4.3 Depletion of Ninein does not affect microtubule nucleation at the early stage, but causes decreased microtubule density at the late stage of microtubule regrowth.

While the importance of Ninein in microtubule anchoring has been extensively reported and confirmed, the same cannot be said about its role in microtubule nucleation. While several studies propose that Ninein is involved in nucleation by recruiting γ-TuRC to the centrosome, experiments conducted on epithelial cells suggest that Ninein is exclusively involved in anchoring and minus-end capping (Delgehyr et al., 2005; Lin et al., 2006; Mogensen et al., 2000; Piel et al., 2000). We thus decided to investigate whether Ninein functions in microtubule nucleation. To this end, we performed a microtubule regrowth assay on RPE 4KO cells treated with Nocodazole and depleted of Ninein through RNA interference. After 30 seconds of microtubule regrowth, we could not observe clear differences between control and treated cells (Figure 6A and 6B); on the other hand, microtubule density appeared decreased in Ninein-depleted cells after 2 minutes of microtubule regrowth (Figure 6C and 6D). At 30 seconds, the main activity taking place in the cells is microtubule nucleation. Considering that at this stage microtubule regrowth was not impaired in Ninein knock down cells, we hypothesize that Ninein is not involved in the process of nucleation. On the other hand, we assume that microtubules are not only nucleated, but also anchored, after 2 minutes of regrowth. As at this stage we could detect a decreased microtubule density in Ninein-depleted cells, this experiment also suggests that the presence of Ninein is required for proper anchoring of microtubules.

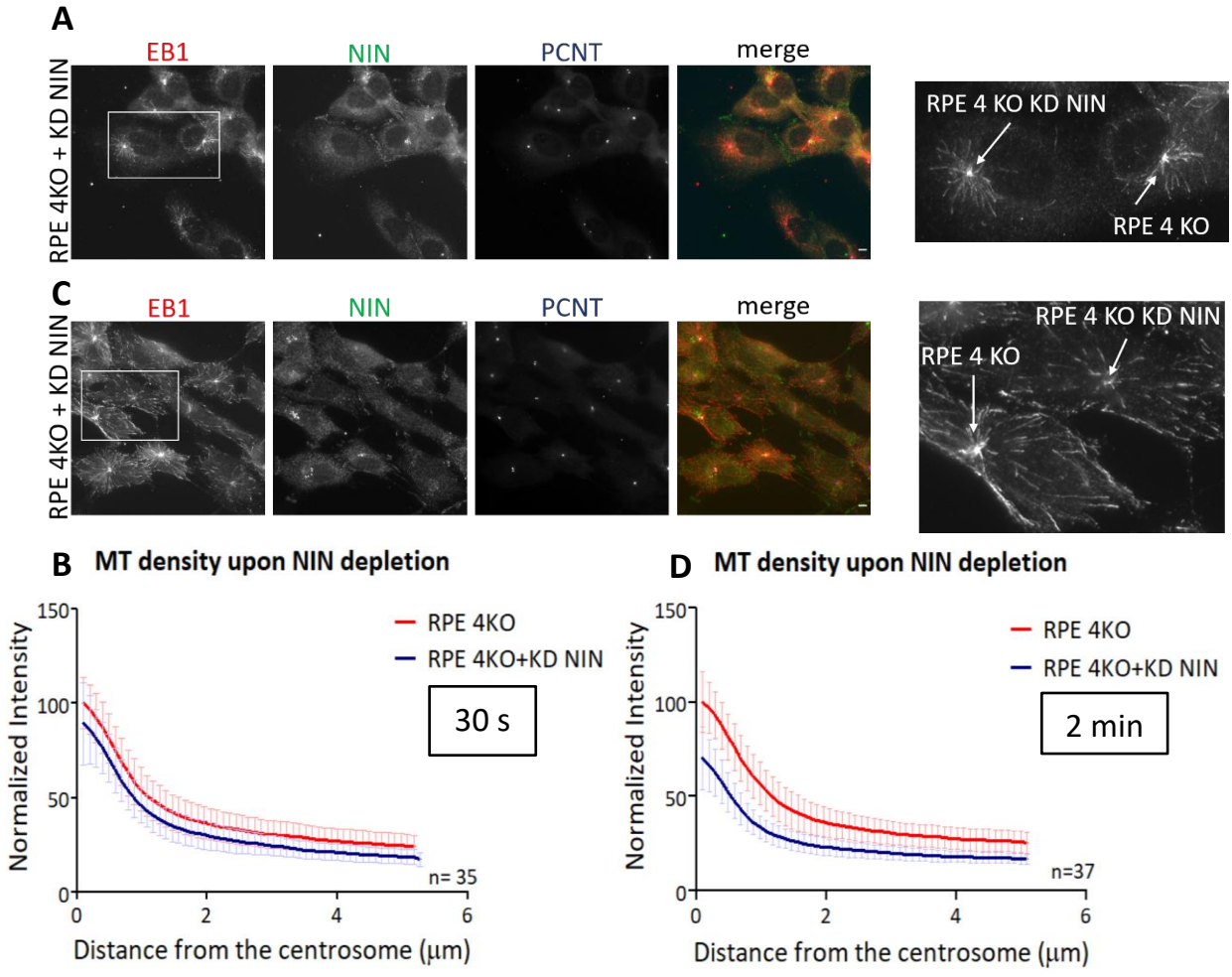

Figure 6. Ninein depletion impairs microtubule density at the late stage of microtubule regrowth, but does not affect nucleation at the early stage.

A. Immunofluorescence staining showing microtubule regrowth after 30 seconds in control and Ninein depleted cells. To avoid any accidental error related to time differences, control and NIN KD cells were mixed before performing the regrowth assay. Cells were stained for microtubule plus-ends (EB1, red), Ninein (green) and centrosomal marker PCNT (blue). On the right, a detail showing the control and NIN KD cells. **B**. Graph showing no significant difference in microtubule nucleation upon Ninein depletion at 30 seconds. Fiji Radial Intensity plug-in was used for this quantification. 35 cells per condition were analyzed. **C**. Same as A, but after 2 minutes of microtubule regrowth. On the right, a detail showing the difference between control and NIN KD cells. **D**: Same as B, but after 2 minutes of microtubule regrowth. The difference between control and treated cells is significant ($p<0.0001$, t test). In panels A and C, scale bars represent 5 µm. In panels B and D, bars represent SD.

4.4 Ninein depletion does not affect γ-tubulin at the centrosome and relocated Ninein does not recruit γ-tubulin.

Many PCM proteins involved in microtubule nucleation at the centrosome, such as PCNT, NEDD1, AKAP9 and CDK5RAP2 are able to recruit and (in some cases) activate γ-TuRC (Paz and Lüders, 2018). We speculated that if Ninein was involved in nucleation, it should be able to interact with γ-TuRC as well. For this reason, we tested whether depleting Ninein from the centrosome would affect γ-tubulin. However, no visible differences in the levels of γ-tubulin at the centrosome could be found between RPE NIN KO cells and control cells (Figure 7A). We repeated the same experiment in RPE 4KO cells depleted of Ninein via siRNA; again, depletion of Ninein did not affect centrosomal γ-tubulin (Figure 7B and C). Finally, we tried to assess if any interaction between Ninein and γ-tubulin could take place by relocating Ninein FL to the *cis* Golgi surface and by checking if γ-tubulin would be recruited to the same cellular compartment because of the interaction with Ninein. In order to recruit Ninein to the Golgi apparatus, we fused Ninein FL to AKAP9 N-terminal domain, the region that is responsible for its localization at the Golgi. RPE AKAP9 -/-, CAMSAP2 -/- cells (RPE 2KO) were transfected with the GFP-AKAP91-1029^NIN FL plasmid and fixed 24 hours later. In contrast to Ninein, which was successfully recruited to the Golgi, γ-tubulin remained localized exclusively to the centrosome (Figure 7D). We concluded that Ninein and γ-tubulin are not involved in interactions at the centrosome. This result was confirmed by analysis of Ninein's interactome through Mass Spectrometry (Figure 7E), where γ-tubulin was found very low-ranked, suggesting an indirect interaction with Ninein.

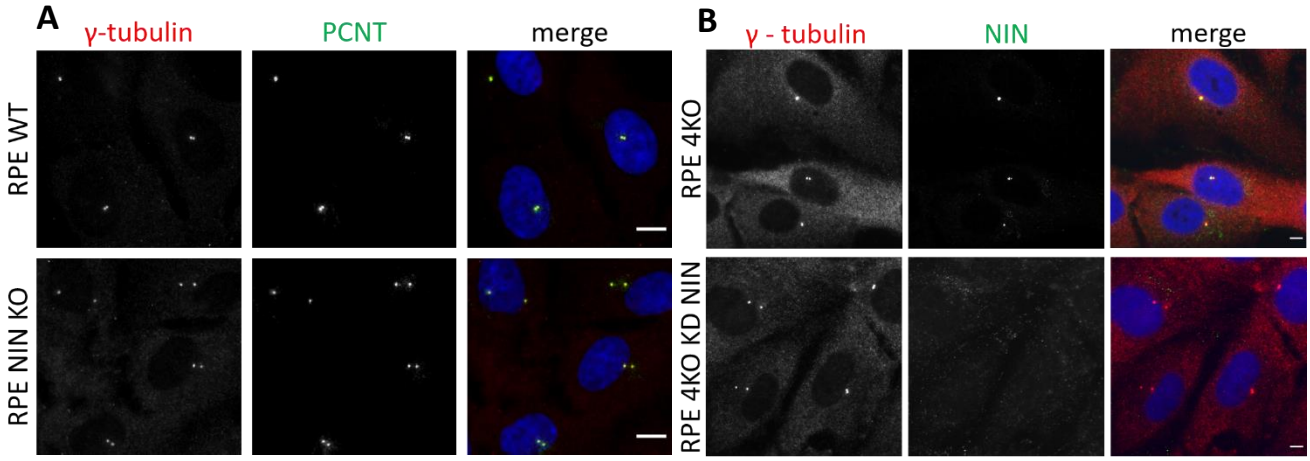

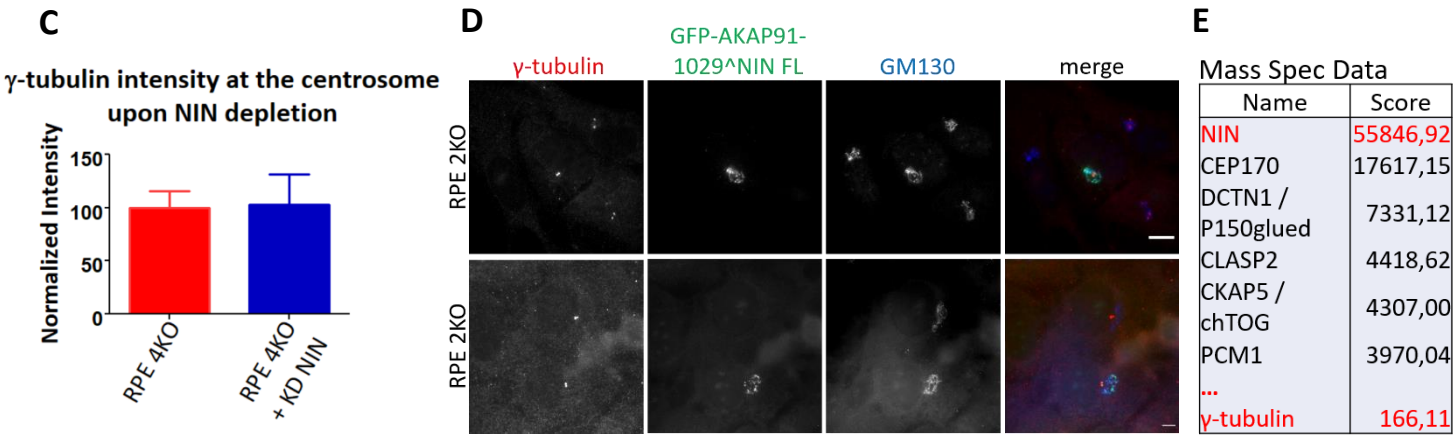

Figure 7. Ninein and γ-tubulin do not interact with each other.

A: Immunofluorescence staining showing γ-tubulin levels at the centrosome in RPE WT and NIN KO cells. Cells were stained for γ-tubulin (red), centrosomal marker PCNT (green) and DAPI (blue). **B**: Immunofluorescence staining showing that depletion of Ninein in RPE 4KO does not affect γ-tubulin levels at the centrosome. Cells were stained for γ-tubulin (red), Ninein (green) and DAPI (blue). **C**: Histogram showing that γ-tubulin levels at the centrosome are equal in RPE 4KO and 4KO KD NIN. 50 cells for each condition were analyzed. Bars represent SD. **D**: Immunofluorescence staining showing that relocated Ninein does not recruit γ-tubulin at the cis Golgi surface. Cells were stained for γ-tubulin (red) and Golgi marker GM130 (blue). Scale bars represent 5 µm. **E**: Summary of Mass Spectrometry analysis of Ninein's partners. For each protein, the score is also reported.

4.5 Ninein interacts with CLASP2 through its 601-1050 coiled-coil domain.

One of the highest-ranked proteins in our Mass Spectrometry analysis of Ninein's interactome was the centrosomal- and Golgi-resident protein CLASP2. As we previously found that the levels of CLASP2 at the centrosome are dramatically decreased in RPE NIN KO cells (Figure 8A), we decided to study more into detail the relationship between Ninein and CLASP2. To this end, we performed a series of Pull-Down assays with streptavidin-coated beats in order to map in detail the respective regions that in these two proteins are responsible for the interaction. The first Pull-Down experiment was performed after overexpressing eight biotinylated Ninein truncations (baits, Figure 8B) and GFP-CLASP2 full length (prey) in HeK 293T cells. We observed that the five Ninein truncations able to bind CLASP2 FL shared the 601-1050 amino acidic region, and that therefore it was probable that this domain was responsible for the interaction with CLASP2 (Figure 8B and 8C).

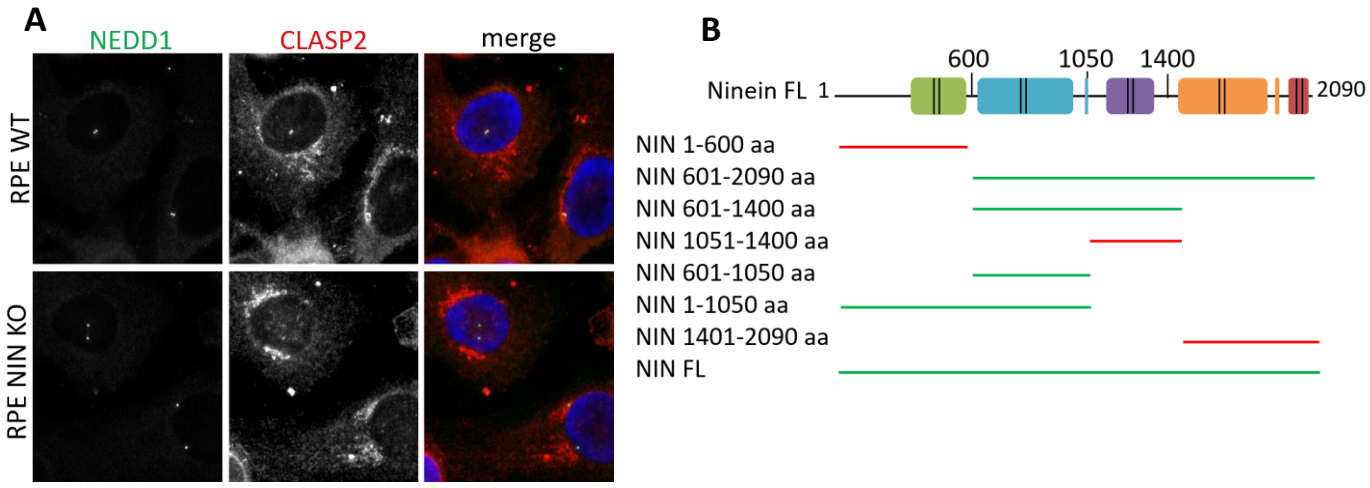

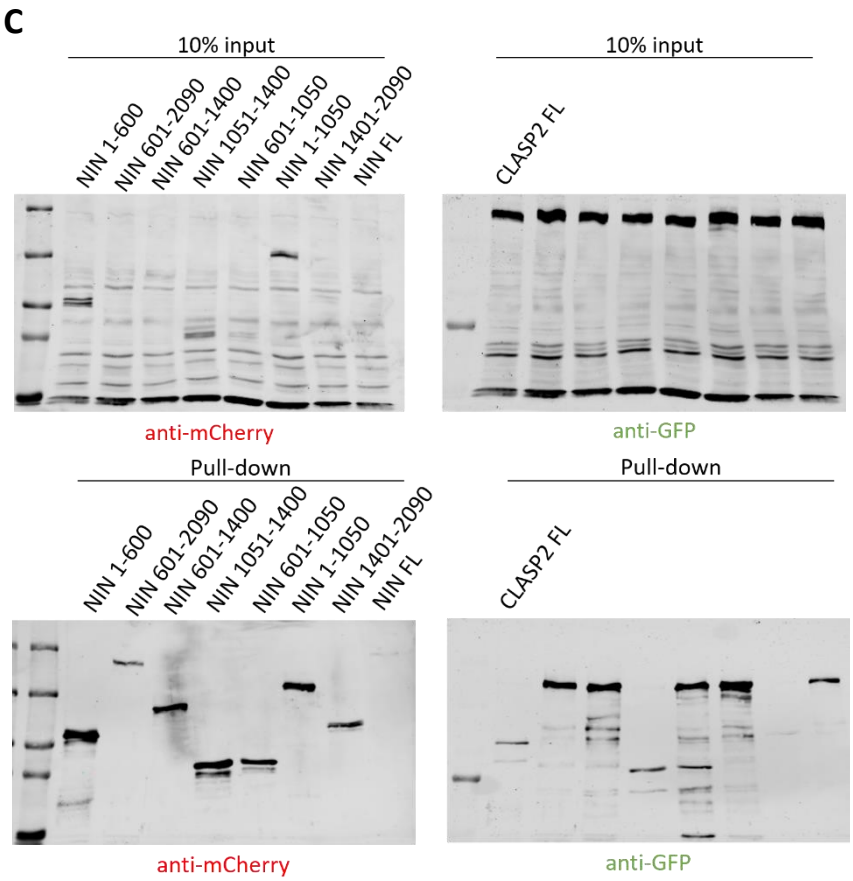

Figure 8. Ninein binds to CLASP2 through its 601-1050 amino acidic region.

A: Immunofluorescence staining showing decreased centrosomal levels of CLASP2 in RPE NIN KO cells. NEDD1 (green) was used as a centrosomal marker. **B**: Schematic representation of the Ninein truncations used in the Pull-Down experiment. The truncations able to pull-down CLASP2 are represented in green, whereas the ones that did not interact with CLASP2 are shown in red. **C**: Western Blots showing the result of the Pull-Down experiment. Bio-TEV-mCherry-Ninein truncations were used as preys and probed in the Western Blot with an anti-mCherry antibody, whereas GFP-CLASP2 FL was used as bait and probed with an anti-GFP antibody. Both the Input and Pull-Down samples are shown.

4.6 Ninein 830-893 coiled-coil domain is responsible for the interaction with CLASP2.

After having identified the 601-1050 amino acidic region in Ninein as responsible for the interaction with CLASP2, we decided to map more precisely the Ninein residues that are primarily involved in the binding process. We noted that a stretch of 10 amino acids (800-809 amino acidic region), contained in the 766-809 coiled-coil domain and able to form a loop, was particularly conserved among different species (not shown). This led us to think that these residues are involved in the interaction with CLASP2. To test this hypothesis, we performed another Pull-Down assay with GFP-CLASP2 as prey and new Ninein truncations, lacking the loop or the 766-809 coiled-coil domain (represented in Figure 9B) as baits (Figure 9A and B). Surprisingly, two Ninein truncations lacking the loop or the coiled-coil domain were able to precipitate CLASP2, while the truncation containing only the 766-809 coiled-coil domain was not enough to bind to the prey. The Pull-Down assay demonstrated that nor the 766-809 coiled-coil domain or the 800-809 loop are involved in the interaction with CLASP2 and that the N-terminal or C-terminal region of the 601-1050 domain are as well not sufficient to guarantee the binding between Ninein and CLASP2. However, we observed that all the Ninein truncations able to pull-down CLASP2 shared the 833-882 coiled-coil domain, suggesting that this region could be important in the binding process. We were able to confirm this by performing a third Pull-Down assay,

where we successfully precipitated GFP-CLASP2 FL with Bio-TEV-mCherry Ninein 830-893 (Figure 9C and D). Removing this coiled-coil domain disrupted Ninein-CLASP2 interaction, confirming that indeed the 833-882 region in Ninein is required and sufficient for the binding with CLASP2.

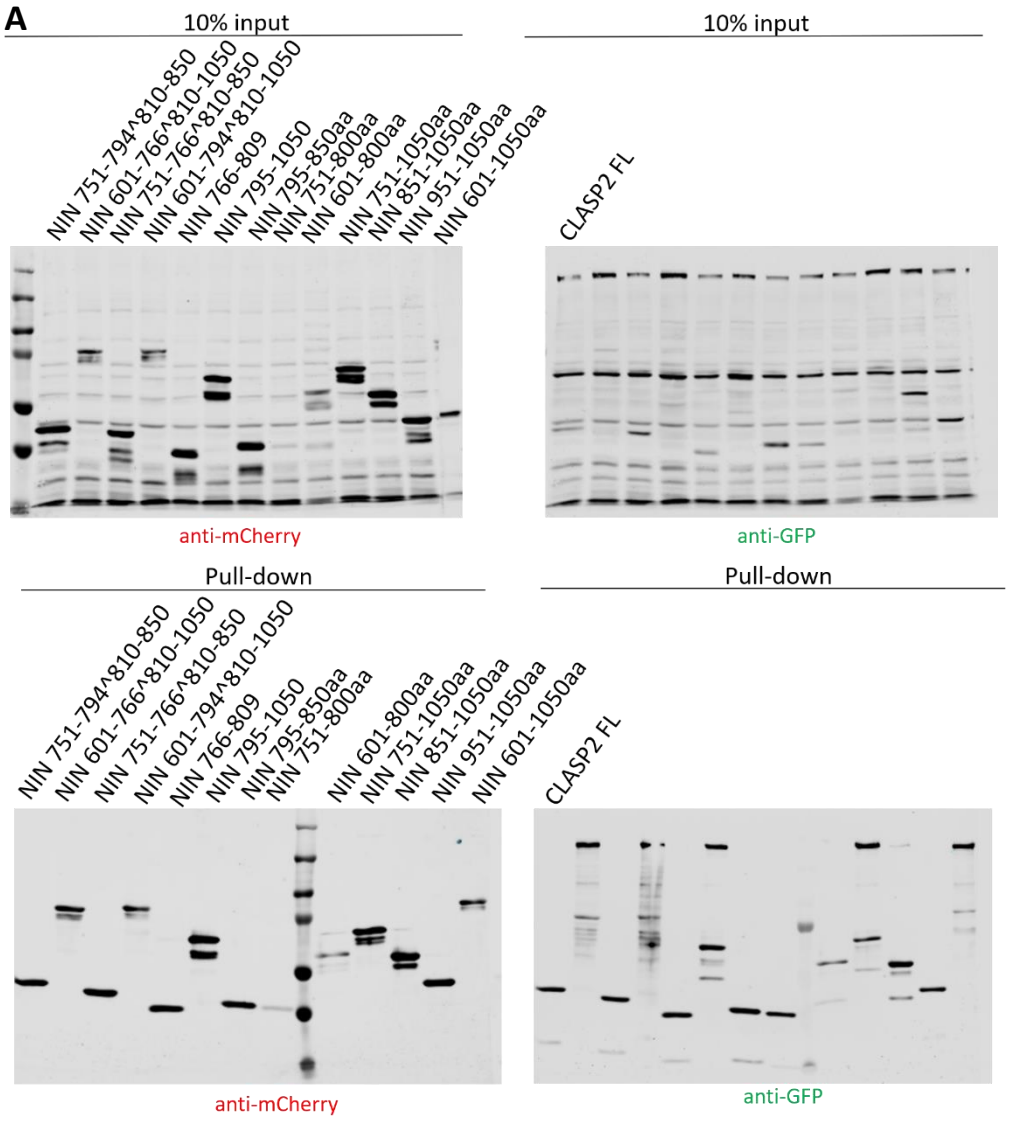

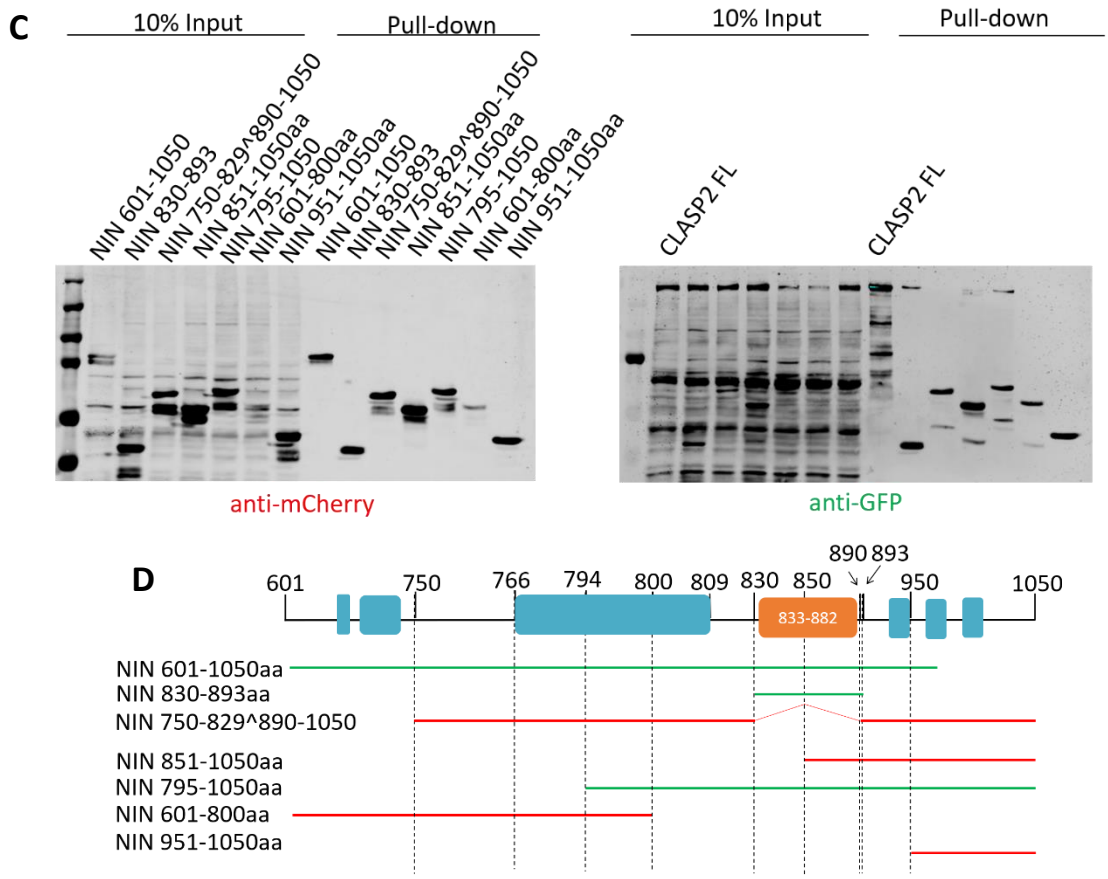

Figure 9. Ninein 830-893 coiled-coil domain is responsible for the interaction with CLASP2

A/C: Western Blots showing the result of the Pull-Down experiments. Bio-TEV-mCherry-Ninein truncations were used as preys and probed in the Western Blot with an anti-mCherry antibody, whereas GFP-CLASP2 FL was used as bait and probed with a anti-GFP antibody. Both the Input and Pull-Down samples are shown. **B/D**: Schematic representations of the Ninein truncations used in the Pull-Down experiments (A and C respectively). The truncations able to pull-down CLASP2 are represented in green, whereas the ones that did not interact with CLASP2 are shown in red.

4.7 CLASP2 interacts with Ninein through the C-terminal CLIP-ID domain.

We concluded mapping the Ninein-CLASP2 interaction by testing which of the four domains of CLASP2 (TOG1, TOG2, TOG 3 and CLIP-ID) is involved in the binding with Ninein. To this end, we overexpressed Bio-TEV-mCherry Ninein 601-1050 as bait and seven GFP-CLASP2 truncations as preys in Hek293T cells and performed one last Pull-Down assay (Figure 10 A and B). The only CLASP2 truncations pulled-down by Ninein where the ones containing the C-terminal CLIP-ID domain. Therefore, we concluded that the CLASP2 1120-1527 amino acidic region is the one interacting with Ninein.

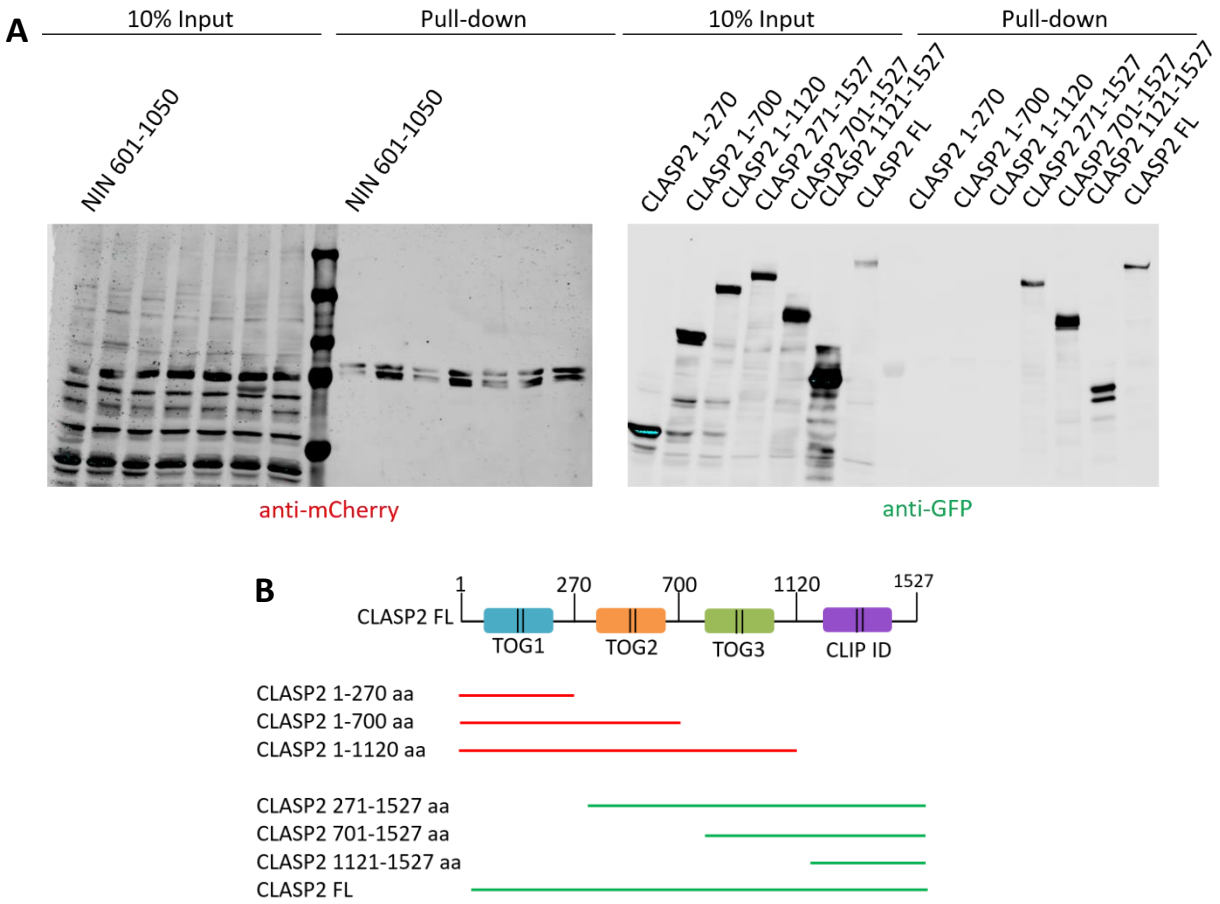

Figure 10. CLASP2 interacts with Ninein through its CLIP-ID domain.

A: Western Blots showing the result of the Pull-Down experiment. Bio-TEV-mCherry-Ninein 601-1050 was used as prey and probed in the Western Blot with an anti-mCherry antibody, whereas GFP-CLASP2 truncations were used as baits and probed with an anti-GFP antibody. Both the Input and Pull-Down samples are shown. **B**: Schematic representation of the CLASP2 truncations used in the Pull-Down experiment. The truncations pulled-down by Ninein are represented in green, whereas the ones that did not interact with the prey are shown in red.

5. Discussion

In this report we investigated the role of Ninein in the regulation of microtubule organization at the centrosome, focusing in particular on its contribution in the processes of microtubule nucleation and anchoring. Although it is known that this protein plays a key role in the formation of a normal radial microtubule array at the centrosome, it remains to be determined whether Ninein is involved in the formation of new microtubules, or if its function is strictly confined to ensuring their proper anchoring. We found that Ninein is recruited to the centrosome through its C-terminal domain, and that its depletion severely impairs the normal microtubule density at the centrosome. Moreover, we observed that Ninein and γ-tubulin do not interact, and that γ-tubulin levels at the centrosome are not affected by Ninein's depletion. We tested microtubule nucleation in Ninein knock-down cells, and found that the late stage of microtubule regrowth, but not the early one, is impaired in the absence of Ninein. Finally, we demonstrated that CLASP2 levels at the centrosome are dramatically decreased upon Ninein depletion, and that Ninein binds to the C-terminal region of CLASP2 trough a coiled-coil domain located in the 601-1050 amino acidic region.

We found that Ninein localization at the centrosome is mediated by its C-terminal domain (1401-2090 amino acidic region). In particular, the amino acidic region located between amino acids 1897 and 2090 was sufficient to target Ninein to the centrosome, whereas both the N-terminal domain and the coiled-coil rich central region of the protein remained diffused in the cytoplasm. Consistent with this result, Delgehyr and coworkers (Delgehyr et al., 2005) showed that the centrosomal targeting domain is located in the C-terminal region (1874-2113 amino acidic region) of mouse Ninein, whereas the N-terminal domain is required to recruit Ninein exclusively at the mother centriole. Ninein was also found to localize at the centrosome through the C-terminal domain by Chen *et al*., (Chen et al., 2003), who identified the minimal binding domain in the 1617-1699 amino acidic region. However, other regions, such as the Leucine zippers in the central domain (1291-1575 amino acidic region) and the N-terminal domain, were reported as responsible for Ninein targeting at the centrosome (respectively, Lin et al., 2006; Stillwell et al., 2004). Therefore, a consensus on the centrosomal targeting domain is lacking, and further studies are needed to clearly identify which domain is responsible for Ninein centrosomal localization. Of note, Ninein seems to possess a particular centrosomal targeting domain, as it was previously shown that this protein does not contain the PACT domain, a specific protein region that targets both PCNT and AKAP9 to the centrosome (Chen et al., 2003). Another aspect that remains to be clarified is whether Ninein could act as a dimer. Indeed, several papers have shown that Ninein can oligomerize, and purification of the full-length version as well as the C-terminal domain of the protein has proved to be difficult in many cases (Casenghi et al., 2005; Chen et al., 2003; Delgehyr et al., 2005; Wang et al., 2015). Moreover, Ninein's protein structure is characterized by only one EF hand, a motif that is usually present in multiples of two in proteins (Bouckson-Castaing et al., 1996). It is therefore plausible that multiple EF hands might be important to mediate the association of multiple copies of the Ninein protein, although more detailed studies are required to demonstrate whether this is truly happening.

Our observation that Ninein depletion decreases the normal microtubule density at the centrosome points to Ninein being necessary in the process of microtubule anchoring. Additional substantial evidences for this hypothesis are presented in previous studies demonstrating that knock-down of Ninein or antibodies microinjections targeting Ninein induced disorganized and unanchored microtubules, whereas Ninein overexpression is associated with increased retention of microtubules at the centrosome (Abal et al., 2002; Dammermann and Merdes, 2002; Delgehyr et al., 2005; Ibi et al., 2011; Ou et al., 2002). Moreover, Piel and coworkers showed that a dense array of microtubules can only be observed on the Ninein-enriched mother centriole. (Piel et al., 2000). Consistently, after

nocodazole treatment, only the mother centriole is able to anchor the newly formed microtubule array. Although there is agreement on the importance of Ninein in microtubule anchorage, the mechanism behind this process remains to be explained. In particular, it is not clear whether Ninein could bind to microtubules minus-ends directly, or if its anchoring capacity is dependent on additional factors such as γ-TuRC. As we could not detect any direct interaction between Ninein and the minus-ends in *in vitro* experiments (not shown), it is likely that the presence of Ninein itself is not enough to guarantee the attachment of microtubules at the centrosome. However, studies conducted on epithelial cells might show that Ninein binds to minus-ends to mediate their release and anchoring (Mogensen et al., 2000). In cochlear supporting epithelial cells, where anchoring of microtubule takes place at apical sites which do not contain the centrosome, Ninein was in fact seen moving similarly to the newly formed microtubules, which are transported from their centrosomal nucleation site to the apical anchoring site (Mogensen et al., 2000). This suggests that Ninein-containing anchoring complexes are transported together with newly nucleated microtubules, possibly through the mediation of the minus-end directed motor dynein (Casenghi et al., 2005). In this scenario, Ninein could represent not only an anchoring factor, but a stabilizing minus-end binding protein as well. The position of Ninein on the proximal end of the centriole, where the minus-ends of the centriole microtubules are located, could itself be considered as a proof for Ninein's minus-end binding properties (Mogensen et al., 2000). Nevertheless, evidences of Ninein binding to microtubules have been reported both in epithelial cells and in *in vitro* studies performed on the *C.elegans* homolog of Ninein, NOCA-1 (Moss et al., 2007; Wang et al., 2015). It is interesting to note that in the epidermis of larval and adult *C.elegans*, NOCA-1 operates redundantly to PATRONIN, the homolog of the minus-end binding proteins CAMSAPs (Wang et al., 2015). Therefore, it would be interesting to investigate whether Ninein is indeed able to interact with minus-ends, and whether Ninein and CAMSAPs also act in parallel to anchor and stabilize minus ends in mammalian cells. This could be done, for example, by employing live imaging microscopy to follow the processes of microtubule nucleation and release in the presence of GFP-tagged Ninein.

Ninein has also been described as a possible factor involved in the regulation of microtubule nucleation, possibly by promoting the recruitment of γ-tubulin at the centrosome. Several papers reported that the levels of Ninein expression correlate with those of γ-tubulin and that the overexpression of Ninein leads to the formation of cytoplasmic agglomerates where γ-tubulin is also present (Delgehyr et al., 2005; Lin et al., 2006; Stillwell et al., 2004). The interaction between γ-tubulin and Ninein has been previously demonstrated through immunoprecipitation, and, consistently, it has been observed that the depletion of Ninein leads to reduced amounts of γ-tubulin at the centrosome (Delgehyr et al., 2005; Lin et al., 2006). By showing that cells transfected with the C-terminal domain of Ninein display delayed nucleation and dispersed γ-tubulin, Delgehyr and colleagues (Delgehyr et al., 2005) proposed that Ninein promotes microtubule nucleation by recruiting γ-tubulin to the centrosome through its N-terminal domain. This theory is supported by the evidence that Ninein-like-protein, which shares the N-terminal region of Ninein, is able to interact with γ-tubulin and GCP4 of the γ-TuRC complex (Casenghi et al., 2003). In contrast with these observations, we showed that the levels of γ-tubulin at the centrosome are not affected by the depletion of Ninein and that relocated Ninein does not interact with γ-tubulin. This suggests that the recruitment of γ-TuRC at the centrosome is not dependent on Ninein. Consistently, γ-tubulin appeared as a low-scored protein in our mass spectrometry analysis of Ninein's interactome, meaning either that the interaction between the two proteins is indirect or that the interaction is not taking place. We as well tried to pull down endogenous γ-tubulin with biotinylated Ninein, but we failed, possibly because of Ninein full length being insoluble or prone to aggregation. Interestingly, when performing microtubule regrowth assay on knock-down Ninein cells, we observed that microtubule density at the late regrowth stage, but not microtubule nucleation activity at the early regrowth stage, was impaired. At the early stage of

microtubule regrowth, when the concentration of tubulin is high, the only process taking place is microtubule nucleation. Thus, as no difference was detected between Ninein-depleted cells and control cells, we hypothesize that Ninein is not involve in the regulation of microtubule nucleation. On the other hand, it is reasonable to assume that after two minutes of microtubule regrowth, processes like microtubule anchoring and release are fully active. Knock-down Ninein cells showed a reduced microtubule density at this stage, suggesting that the presence of this protein is required for proper microtubule anchoring and release. Altogether, our results show that Ninein is a centrosomal protein which plays a crucial role in anchoring and release of microtubule, but that is not involved in microtubule nucleation. This model is in accordance with the work performed on cochlear epithelial cells by Mogensen and colleagues (Mogensen et al., 2000; Piel et al., 2000), who described Ninein as a minus end capping protein able to anchor microtubules and lacking any nucleating-inducing ability. By showing that Ninein, but not γ-tubulin or other nucleating factors, is associated with newly made microtubules in transit from the centrosome to their apical anchoring sites, the authors proposed that microtubule nucleation and anchoring are regulated separately and by different complexes.

One of the proteins found in our Mass Spectrometry analysis of Ninein's interactome was the centrosome- and Golgi-associated protein CLASP2. This result, together with the observation that CLASP2 levels at the centrosome are dramatically decreased in RPE NIN KO cell line, led us to investigate the interaction between Ninein and CLASP2. We found that Ninein interacts with CLASP2 through a coiled-coil domain located inside the 601-1050 amino acidic region, and that the CLIP-ID C-terminal domain of CLASP2 is responsible for this interaction. This result is consistent with previous studies showing that the binding between CLASP and most interactors is mediated by the C-terminal domain (Akhmanova et al., 2001; Efimov et al., 2007; Lansbergen et al., 2006). It is also of note that similarly to what we found with Ninein, CLASP2 often interacts with coiled-coil regions in its partners (Akhmanova et al., 2001; Lansbergen et al., 2006). Ninein and CLASP2 have been found interacting with each other in mitotic cells, although it was reported that in this case Ninein acts downstream of CLASP2 (Logarinho et al., 2012; Maffini et al., 2009). As our findings suggest the opposite (centrosomal location of CLASP2 at the centrosome is dependent on Ninein), it is possible that the dynamics between the two proteins change in different phases of the cell cycle. In the future, it will be important to determine the functional relationship between Ninein and CLASP2, and in particular whether Ninein's anchoring activity at the centrosome is mediated by CLASP2. CLASPs are able to prevent catastrophe of microtubules and to facilitate their rescue (Ambrose et al., 2011; Bouchet et al., 2016; Mimori-Kiyosue et al., 2005). Interestingly, we observed in previous experiments in our lab that Ninein is able to localize to the microtubule lattice in the presence of CLASP2, and that Ninein might be able to slide on microtubules. Therefore, it would be interesting to test if Ninein can also affect microtubule dynamics by performing *in vitro* experiments in the presence of Ninein and CLASP2.

In conclusion, the results shown in this report contributed to the understanding of the role of Ninein in the regulation of microtubule organization at the centrosome. Although many aspects in this topic still remain to be clarified, important information will be obtained in the future by studying the relationship between Ninein and its interactome found through Mass Spectrometry, and by combining experiments in cells with live imaging and *in vitro* approaches.

6. Supplementary

6.1 Supplementary Tables

Target Gene	Primer Sequence
hNIN 751-794^810-850 aa	F1: GAGCTGTACAAGTCCGGACTCAGATCT ACAGAAGAGAAGGTGAGAGGCT R1: GCTTCTATTTGAGAGGTTCtcCTTTGGTGCTTTTCCAAGAGC F2: aGAACCTCTCAAATAGAAGCCCAG R2: CGCGGTACCGTCGACTGCAG TCA CTGTTCCTGGAGGTCCTTCAG
hNIN 751-766^810-850 aa	F1: GAGCTGTACAAGTCCGGACTCAGATCT ACAGAAGAGAAGGTGAGAGGCT R1: GCTTCTATTTGAGAGGTTCTGTGAAACTGCTCTAGTTCCTGAGTC F2: aGAACCTCTCAAATAGAAGCCCAG R2: CGCGGTACCGTCGACTGCAG TCA CTGTTCCTGGAGGTCCTTCAG
hNIN 601-766^810-1050 aa	F1: GAGCTGTACAAGTCCGGACTCA R1: GCTTCTATTTGAGAGGTTCTGTGAAACTGCTCTAGTTCCTGAGTC F2: aGAACCTCTCAAATAGAAGCCCAG R2: GGTACCGTCGACTGCAGAATTCGTCACAGGGCTCCATCTCCTTCCA
hNIN 601-794^810-1050 aa	F1: GAGCTGTACAAGTCCGGACTCA R1: GCTTCTATTTGAGAGGTTCtcCTTTGGTGCTTTTCCAAGAGC F2: aGAACCTCTCAAATAGAAGCCCAG R2: GGTACCGTCGACTGCAGAATTCGTCACAGGGCTCCATCTCCTTCCA
hNIN 766-809 aa	F: GAGCTGTACAAGTCCGGACTCAGATCTCAGGAGCAGCTGACAAGCC R: CGCGGTACCGTCGACTGCAG TCA TCTATTACACTCTGTTTCCATTTTTTCCCTTC
hNIN 795-1050 aa	F: GAGCTGTACAAGTCCGGACTCAGATCT GAGCTTCAGGAGGGAAGGGAA R: CGGTACCGTCGACTGCAG
hNIN 795-850 aa	F: GAGCTGTACAAGTCCGGACTCAGATCT GAGCTTCAGGAGGGAAGGGAA R: CGCGGTACCGTCGACTGCAG TCA CTGTTCCTGGAGGTCCTTCAG
hNIN 751-800 aa	F:GAGCTGTACAAGTCCGGACTCAGATCTACAGAAGAGAAGGTGAGAG GCT R: CGCGGTACCGTCGACTGCAG TCA CCTTCCCTCCTGAAGCTCC
hNIN 601-800 aa	F: GAGCTGTACAAGTCCGGACTCA R: CGCGGTACCGTCGACTGCAG TCA CCTTCCCTCCTGAAGCTCC
hNIN 751-1050 aa	F:GAGCTGTACAAGTCCGGACTCAGATCTACAGAAGAGAAGGTGAGAG GCT R: CGGTACCGTCGACTGCAG
hNIN 851-1050 aa	F: GAGCTGTACAAGTCCGGACTCAGATCT CAGCGTGAGGAGAAATCCCAG R:CGGTACCGTCGACTGCAG
hNIN 951-1050 aa	F: GAGCTGTACAAGTCCGGACTCAGATCT CGTGAGGAGGTCCTGTGC R: CGGTACCGTCGACTGCAG
hNIN 1401-1900 aa	F:CAAGTCCGGACTCAGATCTCGCGGCCGCTTGGAAAAAGTAAAAGCAC ATGAAATTGCC R: TACCGTCGACTGCAGAATTCTTAGGGATTCATGGTACCTGATGGGT
hNIN 1897-2090 aa	F:AGTCCGGACTCAGATCTCGCGGCCGCACCATGAATCCCACAGAGCAA GA

	R:GGTACCGTCGACTGCAGAATTCGTCATTAATGGCAATAAAGGGATGT AAAACTGGAGT
hNIN 750-829^890-1050 aa	F1: GCTGTACAAGTCCGGACTCAgcTGGACAGAAGAGAAGGTGAGAG R1: ATCTCTCTCTCCTGGGTCAGACACCTCTCAGTGACTTTCTG F2: CTGACCCAGGAGAGAGAGAT R2: CGCGGTACCGTCGACTGCAGtcaCAGGGCTCCATCTCCTTCC
hNIN 830-893 aa	F: GCTGTACAAGTCCGGACTCAgcGAAAGCGCTCTGCAAAGCCT R: CGCGGTACCGTCGACTGCAGtcaCTCCTGGGTCAGGACCAGAG
hCLASP2 1-1120 aa	F: GCTGTACAAGTCCGGACTCA GATCT ATGGAGCCCCGCAGCA R: CGCGGTACCGTCGACTGCAG TCA CTGGGTTCCATTGCCAGTG
hCLASP2 1-700 aa	F: GCTGTACAAGTCCGGACTCA GATCT ATGGAGCCCCGCAGCA R: CGCGGTACCGTCGACTGCAG TCA AACTCTTCCTGGAGACCCAGAC
hCLASP2 1-270 aa	F: GCTGTACAAGTCCGGACTCA GATCT ATGGAGCCCCGCAGCA R: CGCGGTACCGTCGACTGCAG TCA ATTTCCGGATGTTTTAGGTGCAG
hCLASP2 1121-1527 aa	GAGCTGTACAAGTCCGGACTCAGATCT AGTTCCATGGGGAGTCCTTTG R: CGCGGTACCGTCGACTGCAG TCA CTAACTTTGTCCAGAAACATCAGT
hCLASP2 701-1527 aa	F: GAGCTGTACAAGTCCGGACTCAGATCT CTGACCACAACAGCCCTGT R:CGCGGTACCGTCGACTGCAG TCA CTAACTTTGTCCAGAAACATCAGT
hCLASP2 271-1527 aa	F: GAGCTGTACAAGTCCGGACTCAGATCT CCTGCCAACAGTGCAAGG R:CGCGGTACCGTCGACTGCAG TCA CTAACTTTGTCCAGAAACATCAGT

Table S1. List of primers used for PCR.

PCR Templates	Bacterial Selection Marker	Mammalian Selection Marker
Bio-Tev mCherry NIN 601-1050 aa	Kanamycin	Neomycin
Bio-Tev mCherry NIN 1401-2090 aa	Kanamycin	Neomycin
StrepII-mCherry-CLASP2 FL	Kanamycin	Neomycin
Vectors	**Bacterial Selection Marker**	**Mammalian Selection Marker**
Bio-Tev mCherry NIN 601-1050 aa	Kanamycin	Neomycin
pEGFP-C1-NIN 601-1050 aa	Kanamycin	Neomycin
Generated Plasmids	**Bacterial Selection Marker**	**Mammalian Selection Marker**
Bio-Tev-mCherry-NIN 751-794^810-850 aa	Kanamycin	Neomycin
Bio-Tev-mCherry-NIN 601-766^810-1050 aa	Kanamycin	Neomycin
Bio-Tev-mCherry-NIN 751-766^810-850 aa	Kanamycin	Neomycin
Bio-Tev-mCherry-NIN 601-794^810-1050 aa	Kanamycin	Neomycin
Bio-Tev-mCherry-NIN 766-809 aa	Kanamycin	Neomycin
Bio-Tev-mCherry-NIN 794-1050 aa	Kanamycin	Neomycin
Bio-Tev-mCherry-NIN 794-850 aa	Kanamycin	Neomycin
Bio-Tev-mCherry-NIN 751-800 aa	Kanamycin	Neomycin
Bio-Tev-mCherry-NIN 601-800 aa	Kanamycin	Neomycin
Bio-Tev-mCherry-NIN 751-1050 aa	Kanamycin	Neomycin
Bio-Tev-mCherry-NIN 851-1050 aa	Kanamycin	Neomycin
Bio-Tev-mCherry-NIN 951-1050 aa	Kanamycin	Neomycin
EGFP-NIN 1401-1900 aa	Kanamycin	Neomycin
EGFP-NIN 1897-2090 aa	Kanamycin	Neomycin
Bio-Tev-mCherry-NIN 830-893 aa	Kanamycin	Neomycin

Bio-Tev-mCherry-NIN 750-829^890-1050 aa	Kanamycin	Neomycin
pEGFP-CLASP2 1-1120 aa	Kanamycin	Neomycin
pEGFP-CLASP2 1-700 aa	Kanamycin	Neomycin
pEGFP-CLASP2 1-270 aa	Kanamycin	Neomycin
pEGFP-CLASP2 1121-1527 aa	Kanamycin	Neomycin
pEGFP-CLASP2 701-1527 aa	Kanamycin	Neomycin
pEGFP-CLASP2 271-1527 aa	Kanamycin	Neomycin

Table S2. List of generated plasmids.

Plasmids (baits)	Bacterial Selection Marker	Mammalian Selection Marker
Bio-Tev-mCherry-NIN FL	Kanamycin	Neomycin
Bio-Tev-mCherry-NIN 1-600 aa	Kanamycin	Neomycin
Bio-Tev-mCherry-NIN 601-2090 aa	Kanamycin	Neomycin
Bio-Tev-mCherry-NIN 601-1400 aa	Kanamycin	Neomycin
Bio-Tev-mCherry-NIN 1051-1400 aa	Kanamycin	Neomycin
Bio-Tev-mCherry-NIN 601-1050 aa	Kanamycin	Neomycin
Bio-Tev-mCherry-NIN 1-1050 aa	Kanamycin	Neomycin
Bio-Tev-mCherry-NIN 1401-2090 aa	Kanamycin	Neomycin
Bio-Tev-mCherry-NIN 751-794^810-850 aa	Kanamycin	Neomycin
Bio-Tev-mCherry-NIN 601-766^810-1050 aa	Kanamycin	Neomycin
Bio-Tev-mCherry-NIN 751-766^810-850 aa	Kanamycin	Neomycin
Bio-Tev-mCherry-NIN 601-794^810-1050 aa	Kanamycin	Neomycin
Bio-Tev-mCherry-NIN 830-893 aa	Kanamycin	Neomycin
Bio-Tev-mCherry-NIN 750-829^890-1050 aa	Kanamycin	Neomycin
Bio-Tev-mCherry-NIN 766-809 aa	Kanamycin	Neomycin
Bio-Tev-mCherry-NIN 795-1050 aa	Kanamycin	Neomycin
Bio-Tev-mCherry-NIN 795-850 aa	Kanamycin	Neomycin
Bio-Tev-mCherry-NIN 751-800 aa	Kanamycin	Neomycin
Bio-Tev-mCherry-NIN 601-800 aa	Kanamycin	Neomycin
Bio-Tev-mCherry-NIN 751-1050 aa	Kanamycin	Neomycin
Bio-Tev-mCherry-NIN 851-1050 aa	Kanamycin	Neomycin
Bio-Tev-mCherry-NIN 951-1050 aa	Kanamycin	Neomycin
Plasmids (preys)	**Bacterial Selection Marker**	**Mammalian Selection Marker**
pEGFP-CLASP2 FL	Kanamycin	Neomycin
pEGFP-CLASP2 1-1120 aa	Kanamycin	Neomycin
pEGFP-CLASP2 1-700 aa	Kanamycin	Neomycin
pEGFP-CLASP2 1-270 aa	Kanamycin	Neomycin
pEGFP-CLASP2 1121-1527 aa	Kanamycin	Neomycin
pEGFP-CLASP2 701-1527 aa	Kanamycin	Neomycin
pEGFP-CLASP2 271-1527 aa	Kanamycin	Neomycin

Table S3. Constructs used for Pull-down assay.

6.2 Supplementary Figures

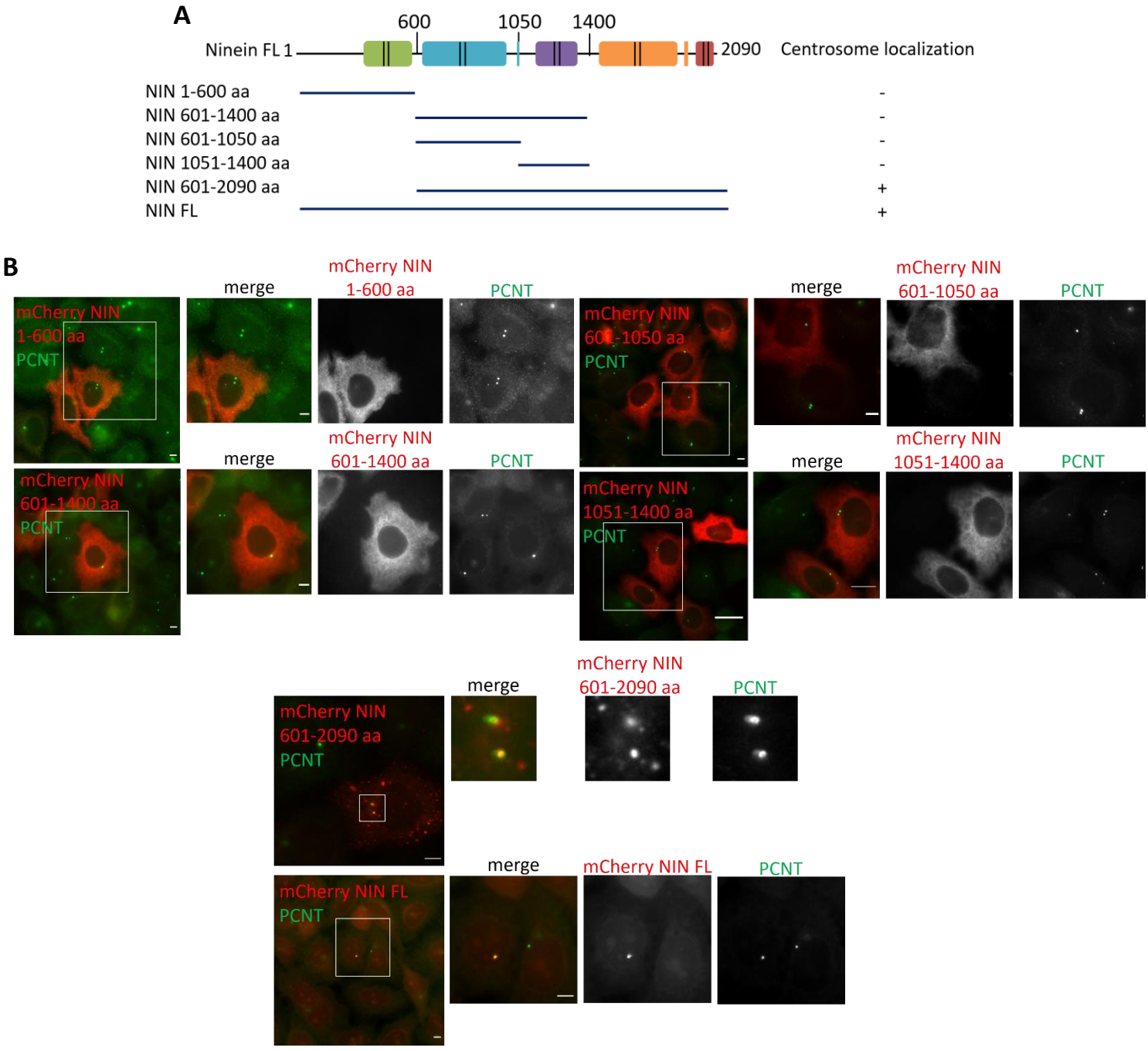

Figure S1. Ninein localization at the centrosome depends on its C-terminal domain.

A. Schematic representation of Ninein truncations used to transfect HeLa cells. Their cellular localization (+: centrosomal; -: cytoplasmic) is shown on the right. **B**. HeLa cells were transfected with the truncations shown in A and fixed 24 hours later. The images, taken at the upright microscope, show Ninein truncations (red) and centrosomal marker PCNT (green).

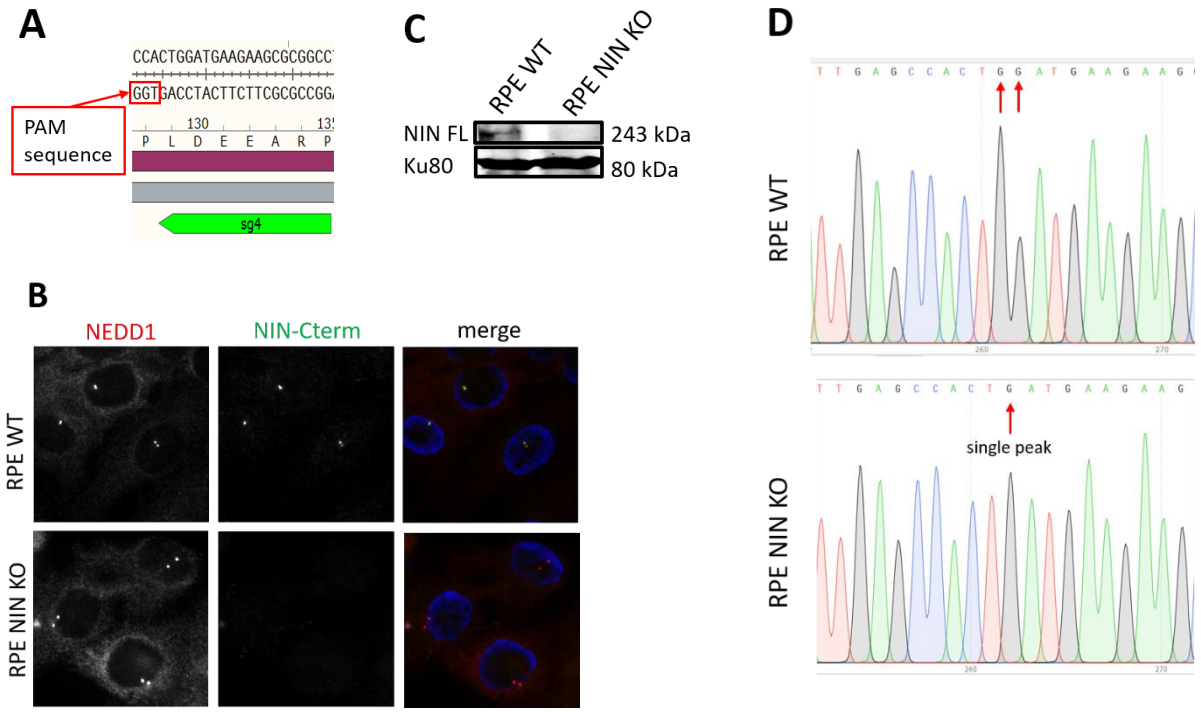

Figure S2. Generation of RPE Ninein KO cell line through CRISPR/Cas9 genome editing technology.

A. sgRNA targeting the N-terminal domain of Ninein used to generate the RPE Ninein KO cell line. **B**. Immunofluorescence staining showing Ninein (green) and centrosomal marker NEDD1 (red) in RPE WT and RPE NIN KO cells. A primary antibody targeting the C-terminal domain of Ninein was used in this case. **C**. Western Blot showing the presence of Ninein in RPE WT and its absence in RPE NIN KO cells. **D**. Sequencing results of the Ninein gene in RPE WT and in RPE NIN KO cells, showing the loss of a guanine in the Knock-out cell line.

7. References

Abal, M., Piel, M., Bouckson-Castaing, V., Mogensen, M., Sibarita, J.B., and Bornens, M. (2002). Microtubule release from the centrosome in migrating cells. J. Cell Biol. *159*, 731–737.

Akhmanova, A., and Steinmetz, M.O. (2015). Control of microtubule organization and dynamics: Two ends in the limelight. Nat. Rev. Mol. Cell Biol. *16*, 711–726.

Akhmanova, A., Hoogenraad, C.C., Drabek, K., Stepanova, T., Dortland, B., Verkerk, T., Vermeulen, W., Burgering, B.M., De Zeeuw, C.I., Grosveld, F., et al. (2001). CLASPs are CLIP-115 and -170 associating proteins involved in the regional regulation of microtubule dynamics in motile fibroblasts. Cell *104*, 923–935.

Ambrose, C., Allard, J.F., Cytrynbaum, E.N., and Wasteneys, G.O. (2011). A CLASP-modulated cell edge barrier mechanism drives cell-wide cortical microtubule organization in Arabidopsis. Nat. Commun. *2*, 1–12.

Anders, A., and Sawin, K.E. (2011). Microtubule stabilization in vivo by nucleation-incompetent γ-tubulin complex. J. Cell Sci. *124*, 1207–1213.

Andersen, J.S., Wilkinson, C.J., Mayor, T., Mortensen, P., Nigg, E.A., and Mann, M. (2003). Proteomic characterization of the human centrosome by protein correlation profiling. Nature *426*, 570–574.

Arquint, C., Gabryjonczyk, A.M., and Nigg, E.A. (2014). Centrosomes as signalling centres. Philos. Trans. R. Soc. B Biol. Sci. *369*.

Askham, J.M., Vaughan, K.T., Goodson, H. V, and Morrison, E.E. (2002). Evidence that an interaction between EB1 and p150(Glued) is required for the formation and maintenance of a radial microtubule array anchored at the centrosome. Mol. Biol. Cell *13*, 3627–3645.

Asteriti, I.A., De Mattia, F., and Guarguaglini, G. (2015). Cross-talk between AURKA and Plk1 in mitotic entry and spindle assembly. Front. Oncol. *5*, 283.

Avidor-Reiss, T., and Gopalakrishnan, J. (2013). Building a centriole. Curr. Opin. Cell Biol. *25*, 72–77.

Azimzadeh, J., and Marshall, W.F. (2010). Building the centriole. Curr. Biol. *20*, R816–R825.

Basto, R., Lau, J., Vinogradova, T., Gardiol, A., Woods, C.G., Khodjakov, A., and Raff, J.W. (2006). Flies without Centrioles. Cell *125*, 1375–1386.

Bornens, M. (2012). The centrosome in cells and organisms. Science (80-.). *335*, 422–426.

Bouchet, B.P., Noordstra, I., van Amersfoort, M., Katrukha, E.A., Ammon, Y.C., ter Hoeve, N.D., Hodgson, L., Dogterom, M., Derksen, P.W.B., and Akhmanova, A. (2016). Mesenchymal Cell Invasion Requires Cooperative Regulation of Persistent Microtubule Growth by SLAIN2 and CLASP1. Dev. Cell *39*, 708–723.

Bouckson-Castaing, V., Moudjou, M., Ferguson, D.J.P., Mucklow, S., Belkaid, Y., Milon, G., and Crocker, P.R. (1996). Molecular characterisation of ninein, a new coiled-coil protein of the centrosome. J. Cell Sci. *109*, 179–190.

Buchman, J.J., Tseng, H.C., Zhou, Y., Frank, C.L., Xie, Z., and Tsai, L.H. (2010). Cdk5rap2 interacts with pericentrin to maintain the neural progenitor pool in the developing neocortex. Neuron *66*, 386–402.

Bugnard, E., Zaal, K.J.M., and Ralston, E. (2005). Reorganization of microtubule nucleation during muscle differentiation. Cell Motil. Cytoskeleton *60*, 1–13.

Casenghi, M., Meraldi, P., Weinhart, U., Duncan, P.I., Körner, R., and Nigg, E.A. (2003). Polo-like kinase 1 regulates Nlp, a centrosome protein involved in microtubule nucleation. Dev. Cell *5*, 113–125.

Casenghi, M., Barr, F.A., and Nigg, E.A. (2005). Phosphorylation of Nlp by Plk1 negatively regulates its dynein-dynactin-dependent targeting to the centrosome. J. Cell Sci. *118*, 5101–5108.

Chabin-Brion, K., Marceiller, J., Perez, F., Settegrana, C., Drechou, A., Durand, G., and Poüs, C. (2001). The Golgi complex is a microtubule-organizing organelle. Mol. Biol. Cell *12*, 2047–2060.

Chen, C.H., Howng, S.L., Cheng, T.S., Chou, M.H., Huang, C.Y., and Hong, Y.R. (2003). Molecular characterization of human ninein protein: Two distinct subdomains required for centrosomal targeting and regulating signals in cell cycle. Biochem. Biophys. Res. Commun. *308*, 975–983.

Choi, Y.K., Liu, P., Sze, S.K., Dai, C., and Qi, R.Z. (2010). CDK5RAP2 stimulates microtubule nucleation by the γ-tubulin ring complex. J. Cell Biol. *191*, 1089–1095.

Cizmecioglu, O., Arnold, M., Bahtz, R., Settele, F., Ehret, L., Haselmann-Weiß, U., Antony, C., and Hoffmann, I. (2010). Cep152 acts as a scaffold for recruitment of Plk4 and CPAP to the centrosome. J. Cell Biol. *191*, 731–739.

Conduit, P.T., Wainman, A., and Raff, J.W. (2015). Centrosome function and assembly in animal cells. Nat. Publ. Gr.

Cota, R.R., Teixidó-Travesa, N., Ezquerra, A., Eibes, S., Lacasa, C., Roig, J., and Lüders, J. (2017). MZT1 regulates microtubule nucleation by linking γTuRC assembly to adapter-mediated targeting and activation. J. Cell Sci. *130*, 406–419.

Dammermann, A., and Merdes, A. (2002). Assembly of centrosomal proteins and microtubule organization depends on PCM-1. J. Cell Biol. *159*, 255–266.

Dauber, A., LaFranchi, S.H., Maliga, Z., Lui, J.C., Moon, J.E., McDeed, C., Henke, K., Zonana, J., Kingman, G.A., Pers, T.H., et al. (2012). Novel microcephalic primordial dwarfism disorder associated with variants in the centrosomal protein ninein. J. Clin. Endocrinol. Metab. *97*, 2140–2151.

Delgehyr, N., Sillibourne, J., and Bornens, M. (2005). Microtubule nucleation and anchoring at the centrosome are independent processes linked by ninein function. J. Cell Sci. *118*, 1565–1575.

Dhani, D.K., Goult, B.T., George, G.M., Rogerson, D.T., Bitton, D.A., Miller, C.J., Schwabe, J.W.R., and Tanaka, K. (2013). Mzt1/Tam4, a fission yeast MOZART1 homologue, is an essential component of the γ-tubulin complex and directly interacts with GCP3Alp6. Mol. Biol. Cell *24*, 3337–3349.

Efimov, A., Kharitonov, A., Efimova, N., Loncarek, J., Miller, P.M., Andreyeva, N., Gleeson, P., Galjart, N., Maia, A.R.R., McLeod, I.X., et al. (2007). Asymmetric CLASP-Dependent Nucleation of Noncentrosomal Microtubules at the trans-Golgi Network. Dev. Cell *12*, 917–930.

Farina, F., Gaillard, J., Guérin, C., Couté, Y., Sillibourne, J., Blanchoin, L., and Théry, M. (2016). The centrosome is an actin-organizing centre. Nat. Cell Biol. *18*, 65–75.

Flor-Parra, I., Iglesias-Romero, A.B., and Chang, F. (2018). The XMAP215 Ortholog Alp14 Promotes Microtubule Nucleation in Fission Yeast. Curr. Biol. *28*, 1681-1691.e4.

Fong, K.W., Choi, Y.K., Rattner, J.B., and Qi, R.Z. (2008). CDK5RAP2 is a pericentriolar protein that functions in centrosomal attachment of the γ-tubulin ring complex. Mol. Biol. Cell *19*, 115–125.

Fry, A.M., Sampson, J., Shak, C., and Shackleton, S. (2017). Recent advances in pericentriolar material organization: Ordered layers and scaffolding gels. F1000Research *6*.

Gavilan, M.P., Gandolfo, P., Balestra, F.R., Arias, F., Bornens, M., and Rios, R.M. (2017). The Centrosome Controls the Number and Spatial Distribution of Microtubules by Negatively Regulating Alternative MTOCs. BioRxiv 153304.

Gillingham, A.K., and Munro, S. (2000). The PACT domain, a conserved centrosomal targeting motif in the coiled-coil proteins AKAP450 and pericentrin. EMBO Rep. *1*, 524.

Gomez-Ferreria, M.A., Bashkurov, M., Helbig, A.O., Larsen, B., Pawson, T., Gingras, A.C., and Pelletier, L. (2012). Novel NEDD1 phosphorylation sites regulate γ-tubulin binding and mitotic spindle assembly. J. Cell Sci. *125*, 3745–3751.

Goodson, H. V., and Jonasson, E.M. (2018). Microtubules and microtubule-associated proteins. Cold Spring Harb. Perspect. Biol. *10*.

Graser, S., Stierhof, Y.D., and Nigg, E.A. (2007a). Cep68 and Cep215 (Cdk5rap2) are required for centrosome cohesion. J. Cell Sci. *120*, 4321–4331.

Graser, S., Stierhof, Y.D., Lavoie, S.B., Gassner, O.S., Lamla, S., Le Clech, M., and Nigg, E.A. (2007b). Cep164, a novel centriole appendage protein required for primary cilium formation. J. Cell Biol. *179*, 321–330.

Guillet, V., Knibiehler, M., Gregory-Pauron, L., Remy, M.H., Chemin, C., Raynaud-Messina, B., Bon, C., Kollman, J.M., Agard, D.A., Merdes, A., et al. (2011). Crystal structure of γ-tubulin complex protein GCP4 provides insight into microtubule nucleation. Nat. Struct. Mol. Biol. *18*, 915–919.

Gunawardane, R.N., Martin, O.C., Cao, K., Zhang, L., Dej, K., Iwamatsu, A., and Zheng, Y. (2000). Characterization and reconstitution of Drosophila γ-tubulin ring complex subunits. J. Cell Biol. *151*, 1513–1523.

Gunawardane, R.N., Martin, O.C., and Zheng, Y. (2003). Characterization of a new γTuRC subunit with WD repeats. Mol. Biol. Cell *14*, 1017–1026.

Gupta, G.D., Coyaud, É., Gonçalves, J., Mojarad, B.A., Liu, Y., Wu, Q., Gheiratmand, L., Comartin, D., Tkach, J.M., Cheung, S.W.T., et al. (2015). A Dynamic Protein Interaction Landscape of the Human Centrosome-Cilium Interface. Cell *163*, 1484–1499.

Hamill, D.R., Severson, A.F., Carter, J.C., and Bowerman, B. (2002). Centrosome maturation and mitotic spindle assembly in C. elegans require SPD-5, a protein with multiple coiled-coil domains. Dev. Cell *3*, 673–684.

Hannak, E., Oegema, K., Kirkham, M., Gönczy, P., Habermann, B., and Hyman, A.A. (2002). The kinetically dominant assembly pathway for centrosomal asters in Caenorhabditis elegans is γ-tubulin dependent. J. Cell Biol. *157*, 591–602.

Haren, L., Remy, M.H., Bazin, I., Callebaut, I., Wright, M., and Merdes, A. (2006). NEDD1-dependent recruitment of the γ-tubulin ring complex to the centrosome is necessary for centriole duplication and spindle assembly. J. Cell Biol. *172*, 505–515.

Hori, A., Ikebe, C., Tada, M., and Toda, T. (2014). Msd1/SSX2IP-dependent microtubule anchorage ensures spindle orientation and primary cilia formation. EMBO Rep. *15*, 175–184.

Hurtado, L., Caballero, C., Gavilan, M.P., Cardenas, J., Bornens, M., and Rios, R.M. (2011). Disconnecting the Golgi ribbon from the centrosome prevents directional cell migration and ciliogenesis. J. Cell Biol. *193*, 917–933.

Hutchins, J.R. a, Toyoda, Y., Hegemann, B., Poser, I., Sykora, M.M., Augsburg, M., Hudecz, O., Buschhorn, B. a, Bulkescher, J., Conrad, C., et al. (2010). Systematic Characterization of Human Protein Complexes Identifies Chromosome Segregation Proteins. Science (80-.). *328*, 593–599.

Ibi, M., Zou, P., Inoko, A., Shiromizu, T., Matsuyama, M., Hayashi, Y., Enomoto, M., Mori, D., Hirotsune, S., Kiyono, T., et al. (2011). Trichoplein controls microtubule anchoring at the centrosome by binding to Odf2 and ninein. J. Cell Sci. *124*, 857–864.

Ishikawa, H., Kubo, A., Tsukita, S., and Tsukita, S. (2005). Odf2-deficient mother centrioles lack distal/subdistal appendages and the ability to generate primary cilia. Nat. Cell Biol. *7*, 517–524.

Jiang, K., Hua, S., Mohan, R., Grigoriev, I., Yau, K.W., Liu, Q., Katrukha, E.A., Altelaar, A.F.M., Heck, A.J.R., Hoogenraad, C.C., et al. (2014). Microtubule minus-end stabilization by polymerization-driven CAMSAP deposition. Dev. Cell *28*, 295–309.

Jurczyk, A., Gromley, A., Redick, S., San Agustin, J., Witman, G., Pazour, G.J., Peters, D.J.M., and Doxsey, S. (2004). Pericentrin forms a complex with intraflagellar transport proteins and polycystin-2 and is required for primary cilia assembly. J. Cell Biol. *166*, 637–643.

Kollman, J.M., Merdes, A., Mourey, L., and Agard, D.A. (2011). Microtubule nucleation by γ-tubulin complexes. Nat. Rev. Mol. Cell Biol. *12*, 709–721.

Kowanda, M., Bergalet, J., Wieczorek, M., Brouhard, G., Léuyer, É., and Lasko, P. (2016). Loss of function of the Drosophila Ninein-related centrosomal protein Bsg25D causes mitotic defects and impairs embryonic development. Biol. Open *5*, 1040–1051.

Lansbergen, G., Grigoriev, I., Mimori-Kiyosue, Y., Ohtsuka, T., Higa, S., Kitajima, I., Demmers, J., Galjart, N., Houtsmuller, A.B., Grosveld, F., et al. (2006). CLASPs Attach Microtubule Plus Ends to the Cell Cortex through a Complex with LL5β. Dev. Cell *11*, 21–32.

Lawo, S., Hasegan, M., Gupta, G.D., and Pelletier, L. (2012). Subdiffraction imaging of centrosomes reveals higher-order organizational features of pericentriolar material. Nat. Cell Biol. *14*, 1148–1158.

Lee, K., and Rhee, K. (2011). PLK1 phosphorylation of pericentrin initiates centrosome maturation at the onset of mitosis. J. Cell Biol. *195*, 1093–1101.

Lin, C.C., Cheng, T.S., Hsu, C.M., Wu, C.H., Chang, L. Sen, Shen, Z.S., Yeh, H.M., Chang, L.K., Howng, S.L., and Hong, Y.R. (2006). Characterization and functional aspects of human ninein isoforms that regulated by centrosomal targeting signals and evidence for docking sites to direct γ-tubulin. Cell Cycle *5*, 2517–2527.

Lin, T.C., Neuner, A., Schlosser, Y., Scharf, A., Weber, L., and Schiebel, E. (2014). Cell-cycle dependent phosphorylation of yeast pericentrin regulates γ-TUSC-mediated microtubule nucleation. Elife *2014*.

Lin, T.C., Neuner, A., Flemming, D., Liu, P., Chinen, T., Jäkle, U., Arkowitz, R., and Schiebel, E. (2016). MOZ ART1 and γ-tubulin complex receptors are both required to turn γ-TuSC into an active microtubule nucleation template. J. Cell Biol. *215*, 823–840.

Logarinho, E., Maffini, S., Barisic, M., Marques, A., Toso, A., Meraldi, P., and Maiato, H. (2012). CLASPs prevent irreversible multipolarity by ensuring spindle-pole resistance to traction forces during chromosome alignment. Nat. Cell Biol. *14*, 295–303.

Lüders, J., Patel, U.K., and Stearns, T. (2006). GCP-WD is a gamma-tubulin targeting factor required for centrosomal and chromatin-mediated microtubule nucleation. Nat. Cell Biol. *8*, 137–147.

Lynch, E.M., Groocock, L.M., Borek, W.E., and Sawin, K.E. (2014). Activation of the γ-tubulin complex by the Mto1/2 complex. Curr. Biol. *24*, 896–903.

Maffini, S., Maia, A.R.R., Manning, A.L., Maliga, Z., Pereira, A.L., Junqueira, M., Shevchenko, A., Hyman, A., Yates, J.R., Galjart, N., et al. (2009). Motor-Independent Targeting of CLASPs to Kinetochores by CENP-E Promotes Microtubule Turnover and Poleward Flux. Curr. Biol. *19*, 1566–1572.

Majewski, F., Ranke, M., and Schinzel, A. (1982). Studies of microcephalic primordial dwarfism II: The osteodysplastic type II of primordial dwarfism. Am. J. Med. Genet. *12*, 23–35.

Manning, J.A., Shalini, S., Risk, J.M., Day, C.L., and Kumar, S. (2010). A Direct Interaction with NEDD1 Regulates γ-Tubulin Recruitment to the Centrosome. PLoS One *5*, e9618.

Martin, M., and Akhmanova, A. (2018). Coming into Focus: Mechanisms of Microtubule Minus-End Organization. Trends Cell Biol. *28*, 574–588.

Masoud, K., Herzog, E., Chabouté, M.-E., and Schmit, A.-C. (2013). Microtubule nucleation and establishment of the mitotic spindle in vascular plant cells. Plant J. *75*, 245–257.

Mazo, G., Soplop, N., Wang, W.J., Uryu, K., and Tsou, M.F.B. (2016). Spatial Control of Primary Ciliogenesis by Subdistal Appendages Alters Sensation-Associated Properties of Cilia. Dev. Cell *39*, 424–437.

Mennella, V., Keszthelyi, B., Mcdonald, K.L., Chhun, B., Kan, F., Rogers, G.C., Huang, B., and Agard, D.A. (2012). Subdiffraction-resolution fluorescence microscopy reveals a domain of the centrosome critical for pericentriolar material organization. Nat. Cell Biol. *14*, 1159–1168.

Mennella, V., Agard, D.A., Huang, B., and Pelletier, L. (2014). Amorphous no more: subdiffraction view of the pericentriolar material architecture. Trends Cell Biol. *24*, 188–197.

Meraldi, P. (2016). Centrosomes in spindle organization and chromosome segregation: a mechanistic view. Chromosom. Res. *24*, 19–34.

Mimori-Kiyosue, Y., Grigoriev, I., Lansbergen, G., Sasaki, H., Matsui, C., Severin, F., Galjart, N., Grosveld, F., Vorobjev, I., Tsukita, S., et al. (2005). CLASP1 and CLASP2 bind to EB1 and regulate microtubule plus-end dynamics at the cell cortex. J. Cell Biol. *168*, 141–153.

Mogensen, M.M., Malik, A., Piel, M., Boukson-Castaing, V., and Bornens, M. (2000). Microtubule minus-end anchorage at Centrosomal and non-centrosomal sites: The role of ninein. J. Cell Sci. *113*, 3013–3023.

Moritz, M., Braunfeld, M.B., Sedat, J.W., Alberts, B., and Agard, D.A. (1995). Microtubule nucleation by γ-tubulin-containing rings in the centrosome. Nature *378*, 638–640.

Moss, D.K., Bellett, G., Carter, J.M., Liovic, M., Keynton, J., Prescott, A.R., Lane, E.B., and Mogensen, M.M. (2007). Ninein is released from the centrosome and moves bi-directionally along microtubules. J. Cell Sci. *120*, 3064–3074.

Mullee, L.I., and Morrison, C.G. (2016). Centrosomes in the DNA damage response—the hub outside the centre. Chromosom. Res. *24*, 35–51.

Muroyama, A., Seldin, L., and Lechler, T. (2016). Divergent regulation of functionally distinct γ-tubulin complexes during differentiation. J. Cell Biol. *213*, 679–692.

Murphy, S.M., Urbani, L., and Stearns, T. (1998). The mammalian γ-tubulin complex contains homologues of the yeast spindle pole body components Spc97p and Spc98p. J. Cell Biol. *141*, 663–674.

Murphy, S.M., Preble, A.M., Patel, U.K., O'Connell, K.L., Prabha Dias, D., Moritz, M., Agard, D., Stults, J.T., and Stearns, T. (2001). GCP5 and GCP6: Two new members of the human γ-tubulin complex. Mol. Biol. Cell *12*, 3340–3352.

Nakagawa, Y., Yamane, Y., Okanoue, T., Tsukita, S., and Tsukita, S. (2001). Outer dense fiber 2 is a widespread centrosome scaffold component preferentially associated with mother centrioles: Its identification from isolated centrosomes. Mol. Biol. Cell *12*, 1687–1697.

Nigg, E.A., and Stearns, T. (2011). The centrosome cycle: Centriole biogenesis, duplication and inherent asymmetries. Nat. Cell Biol. *13*, 1154–1160.

Ohta, T., Essner, R., Ryu, J.-H., Palazzo, R.E., Uetake, Y., and Kuriyama, R. (2002). Characterization of Cep135, a novel coiled-coil centrosomal protein involved in microtubule organization in mammalian cells. J. Cell Biol. *156*, 87–99.

Ou, Y.Y., Mack, G.J., Zhang, M., and Rattner, J.B. (2002). CEP110 and ninein are located in a specific domain of the concentrate associated with centrosome maturation. J. Cell Sci. *115*, 1825–1835.

Paz, J., and Lüders, J. (2018). Microtubule-Organizing Centers: Towards a Minimal Parts List. Trends Cell Biol. *28*, 176–187.

Piel, M., Meyer, P., Khodjakov, A., Rieder, C.L., and Bornens, M. (2000). The respective contributions of the mother and daughter centrioles to centrosome activity and behavior in vertebrate cells. J. Cell Biol. *149*, 317–329.

Pinyol, R., Scrofani, J., and Vernos, I. (2013). The role of NEDD1 phosphorylation by aurora a in chromosomal microtubule nucleation and spindle function. Curr. Biol. *23*, 143–149.

Quintyne, N.J., Gill, S.R., Eckley, D.M., Crego, C.L., Compton, D.A., and Schroer, T.A. (1999). Dynactin is required for microtubule anchoring at centrosomes. J. Cell Biol. *147*, 321–334.

Rauch, A., Thiel, C.T., Schindler, D., Wick, U., Crow, Y.J., Ekici, A.B., Van Essen, A.J., Goecke, T.O., Al-Gazali, L., Chrzanowska, K.H., et al. (2008). Mutations in the pericentrin (PCNT) gene cause primordial dwarfism. Science (80-.). *319*, 816–819.

Redwine, W.B., DeSantis, M.E., Hollyer, I., Htet, Z.M., Tran, P.T., Swanson, S.K., Florens, L., Washburn, M.P., and Reck-Peterson, S.L. (2017). The human cytoplasmic dynein interactome reveals novel activators of motility. Elife *6*.

Reid, T.A., Schuster, B.M., Mann, B.J., Balchand, S.K., Plooster, M., McClellan, M., Coombes, C.E., Wadsworth, P., and Gardner, M.K. (2016). Suppression of microtubule assembly kinetics by the mitotic protein TPX2. J. Cell Sci. *129*, 1319–1328.

Reiter, J.F., and Leroux, M.R. (2017). Genes and molecular pathways underpinning ciliopathies. Nat. Rev. Mol.

Cell Biol. *18*, 533–547.

Rivero, S., Cardenas, J., Bornens, M., and Rios, R.M. (2009). Microtubule nucleation at the cis-side of the Golgi apparatus requires AKAP450 and GM130. EMBO J. *28*, 1016–1028.

Roostalu, J., Cade, N.I., and Surrey, T. (2015). Complementary activities of TPX2 and chTOG constitute an efficient importin-regulated microtubule nucleation module. Nat. Cell Biol. *17*, 1422–1434.

Roubin, R., Acquaviva, C., Chevrier, V., Sedjaï, F., Zyss, D., Birnbaum, D., and Rosnet, O. (2013). Myomegalin is necessary for the formation of centrosomal and Golgi-derived microtubules. Biol. Open *2*, 238–250.

Sanchez, A.D., and Feldman, J.L. (2017). Microtubule-organizing centers: from the centrosome to non-centrosomal sites. Curr. Opin. Cell Biol. *44*, 93–101.

Sánchez, I., and Dynlacht, B.D. (2016). Cilium assembly and disassembly. Nat. Cell Biol. *18*, 711–717.

Sanders, A.A.W.M., and Kaverina, I. (2015). Nucleation and dynamics of Golgi-derived microtubules. Front. Neurosci. *9*, 431.

Sawin, K.E., Lourenco, P.C.C., and Snaith, H.A. (2004). Microtubule nucleation at non-spindle pole body microtubule-organizing centers requires fission yeast centrosomin-related protein mod20p. Curr. Biol. *14*, 763–775.

Schatten, H. (2008). The mammalian centrosome and its functional significance. Histochem. Cell Biol. *129*, 667–686.

Scrofani, J., Sardon, T., Meunier, S., and Vernos, I. (2015). Microtubule nucleation in mitosis by a RanGTP-dependent protein complex. Curr. Biol. *25*, 131–140.

Stillwell, E.E., Zhou, J., and Joshi, H.C. (2004). Human ninein is a centrosomal autoantigen recognized by CREST patient sera and plays a regulatory role in microtubule nucleation. Cell Cycle *3*, 921–928.

Strome, S., Powers, J., Dunn, M., Reese, K., Malone, C.J., White, J., Seydoux, G., and Saxton, W. (2001). Spindle dynamics and the role of γ-tubulin in early Caenorhabditis elegans embryos. Mol. Biol. Cell *12*, 1751–1764.

Sulimenko, V., Hájková, Z., Klebanovych, A., and Dráber, P. (2017). Regulation of microtubule nucleation mediated by γ-tubulin complexes. Protoplasma *254*, 1187–1199.

Sumigray, K.D., and Lechler, T. (2011). Control of cortical microtubule organization and desmosome stability by centrosomal proteins. Bioarchitecture *1*, 221–224.

Takahashi, M., Yamagiwa, A., Nishimura, T., Mukai, H., and Ono, Y. (2002). Centrosomal proteins CG-NAP and kendrin provide microtubule nucleation sites by anchoring gamma-tubulin ring complex. Mol. Biol. Cell *13*, 3235–3245.

Tanaka, N., Meng, W., Nagae, S., and Takeichi, M. (2012). Nezha/CAMSAP3 and CAMSAP2 cooperate in epithelial-specific organization of noncentrosomal microtubules. Proc. Natl. Acad. Sci. U. S. A. *109*, 20029–20034.

Teixidó-Travesa, N., Roig, J., and Lüders, J. (2012). The where, when and how of microtubule nucleation - one ring to rule them all. J. Cell Sci. *125*, 4445–4456.

Thawani, A., Kadzik, R.S., and Petry, S. (2018). XMAP215 is a microtubule nucleation factor that functions synergistically with the γ-tubulin ring complex. Nat. Cell Biol. *20*, 575–585.

Tovey, C.A., and Conduit, P.T. (2018). Microtubule nucleation by γ-tubulin complexes and beyond. Essays Biochem. *62*, 765–780.

Vertii, A., Hehnly, H., and Doxsey, S. (2016). The centrosome, a multitalented renaissance organelle. Cold Spring Harb. Perspect. Biol. *8*, a025049.

Vinogradova, T., Miller, P.M., and Kaverina, I. (2009). Microtubule network asymmetry in motile cells: Role of Golgi-derived array. Cell Cycle *8*, 2168–2174.

Vinogradova, T., Paul, R., Grimaldi, A.D., Loncarek, J., Miller, P.M., Yampolsky, D., Magidson, V., Khodjakov, A., Mogilner, A., and Kaverina, I. (2012). Concerted effort of centrosomal and golgiderived microtubules is required for proper golgi complex assembly but not for maintenance. Mol. Biol. Cell *23*, 820–833.

Walia, A., Nakamura, M., Moss, D., Kirik, V., Hashimoto, T., and Ehrhardt, D.W. (2014). GCP-WD mediates γ-TuRC recruitment and the geometry of microtubule nucleation in interphase arrays of arabidopsis. Curr. Biol. *24*, 2548–2555.

Wang, S., Wu, D., Quintin, S., Green, R.A., Cheerambathur, D.K., Ochoa, S.D., Desai, A., and Oegema, K. (2015). NOCA-1 functions with γ-tubulin and in parallel to Patronin to assemble non-centrosomal microtubule arrays in C. elegans. Elife *4*, 1–34.

Wang, Z., Wu, T., Shi, L., Zhang, L., Zheng, W., Qu, J.Y., Niu, R., and Qi, R.Z. (2010). Conserved motif of CDK5RAP2 mediates its localization to centrosomes and the Golgi complex. J. Biol. Chem. *285*, 22658–22665.

Wang, Z., Zhang, C., and Qi, R.Z. (2014). A newly identified myomegalin isoform functions in Golgi microtubule organization and ER-Golgi transport. J. Cell Sci. *127*, 4904–4917.

Wieczorek, M., Bechstedt, S., Chaaban, S., and Brouhard, G.J. (2015). Microtubule-associated proteins control the kinetics of microtubule nucleation. Nat. Cell Biol. *17*, 907–916.

Wiese, C., and Zheng, Y. (2000). A new function for the γ-tubulin ring complex as a microtubule minus-end cap. Nat. Cell Biol. *2*, 358–364.

Woodruff, J.B., Wueseke, O., and Hyman, A.A. (2014). Pericentriolar material structure and dynamics. Philos. Trans. R. Soc. B Biol. Sci. *369*.

Woodruff, J.B., Wueseke, O., Viscardi, V., Mahamid, J., Ochoa, S.D., Bunkenborg, J., Widlund, P.O., Pozniakovsky, A., Zanin, E., Bahmanyar, S., et al. (2015). Regulated assembly of a supramolecular centrosome scaffold in vitro. Science (80-.). *348*, 808–812.

Woodruff, J.B., Ferreira Gomes, B., Widlund, P.O., Mahamid, J., Honigmann, A., and Hyman, A.A. (2017). The Centrosome Is a Selective Condensate that Nucleates Microtubules by Concentrating Tubulin. Cell *169*, 1066-1077.e10.

Wu, J., and Akhmanova, A. (2017). Microtubule-Organizing Centers. Annu. Rev. Cell Dev. Biol. *33*, 51–75.

Wu, J., de Heus, C., Liu, Q., Bouchet, B.P., Noordstra, I., Jiang, K., Hua, S., Martin, M., Yang, C., Grigoriev, I., et al. (2016). Molecular Pathway of Microtubule Organization at the Golgi Apparatus. Dev. Cell *39*, 44–60.

Young, A., Dictenberg, J.B., Purohit, A., Tuft, R., and Doxsey, S.J. (2000). Cytoplasmic dynein-mediated assembly of pericentrin and γ tubulin onto centrosomes. Mol. Biol. Cell *11*, 2047–2056.

Zhang, X., Chen, M.H., Wu, X., Kodani, A., Fan, J., Doan, R., Ozawa, M., Ma, J., Yoshida, N., Reiter, J.F., et al. (2016). Cell-Type-Specific Alternative Splicing Governs Cell Fate in the Developing Cerebral Cortex. Cell *166*, 1147-1162.e15.

Zheng, Y., Wong, M.L., Alberts, B., and Mitchison, T. (1995). Nucleation of microtubule assembly by a γ-tubulin-containing ring complex. Nature *378*, 578–583.

Zheng, Y., Mennella, V., Marks, S., Wildonger, J., Elnagdi, E., Agard, D., and Megraw, T.L. (2016). The Seckel syndrome and centrosomal protein Ninein localizes asymmetrically to stem cell centrosomes but is not required for normal development, behavior, or DNA damage response in Drosophila. Mol. Biol. Cell *27*, 1740–1752.

Zimmerman, W.C., Sillibourne, J., Rosa, J., and Doxsey, S.J. (2004). Mitosis-specific anchoring of γ tubulin complexes by pericentrin controls spindle organization and mitotic entry. Mol. Biol. Cell *15*, 3642–3657.